FREQUENCY RESPONSE OF FLUID TRANSMISSION LINES WITH A NONLINEAR BOUNDARY CONDITION

By

K. VIJAY KUMAR PILLAI

Bachelor of Engineering
Osmania University
Hyderabad, India
1970

Master of Engineering
Indian Institute of Science
Bangalore, India
1973

Submitted to the Faculty of the Graduate College
of the Oklahoma State University
in partial fulfillment of the requirements
for the Degree of
MASTER OF SCIENCE
December, 1975

Thesis
1975
P641f
cop. 2

OKLAHOMA
STATE UNIVERSITY
LIBRARY

MAR 24 1976

FREQUENCY RESPONSE OF FLUID TRANSMISSION LINES

WITH A NONLINEAR BOUNDARY CONDITION

Thesis Approved:

Karl M. Reed
Thesis Adviser

R F Lowery

Larry D Zirkle

M M Durham
Dean of the Graduate College

935063

This work is respectfully dedicated to my

High School teacher,

Mr. S. J. Reddy

ACKNOWLEDGMENTS

To Dr. Karl N. Reid, I would like to express my deep appreciation for his encouragement of my endeavors and patience with my results. I am particularly indebted to him for his interest, sage advice and the ever-open door that made the timely completion of this thesis possible.

To the members of my committee, Dr. Richard L. Lowery and Dr. Larry D. Zirkle, I would like to express my gratitude for their encouragement and comments.

To Ms. Charlene Fries, I would like to offer my sincere thanks for the excellence of the final draft.

TABLE OF CONTENTS

LIST OF TABLES

LIST OF FIGURES

NOMENCLATURE

a	Inside radius of the line
$a(x)$	Variable defined by Equation (5.4)
A	Maximum flow rate amplitude at x = 0
A_1	Variable defined by Equation (4.14)
A_c	Cross sectional area of the fluid jet at vena-contracta
A_ℓ	Cross sectional area of the line
A_o	Area of the orifice
b	Wall thickness of the conduit
$b(x)$	Variable defined by Equation (5.3)
B	Variable defined by Equation (4.19)
B_1	Variable defined by Equation (4.15)
B_2	Variable defined by Equation (4.25)
B_3	Variable defined by Equation (5.2)
BCP1	Boundary condition parameter for sharp-edged orifice
BCP2	Boundary condition parameter for a short-tube orifice
BCP21	Boundary condition parameter for a sharp-edged inertive orifice
BCP22	Boundary condition parameter for a short-tube inertive orifice
c	Speed of sound in the fluid
$c(x)$	Variable defined by Equation (5.6)
C_c	The ratio (A_ℓ/A_o)

C_d	Coefficient of discharge of the orifice
D	Inside diameter of the line
D_o	Diameter of the circular orifice
e	2.718
E	Modulus of elasticity of the material of the conduit
f	Fluid friction factor
F	Complex constant defined by Equation (C.4)
FN	Frequency number
G	A complex constant defined by Equation (C.17)
H	A complex constant defined by Equation (C.12)
i	$\sqrt{-1}$
J	A complex constant defined by Equation (F.4)
K	A complex constant defined by Equation (F.2)
K'	Variable defined by Equations (3.13) and (3.14)
K_1	Variable defined by Equation (2.6)
K_2	Variable defined by Equation (2.7)
K_3	Isothermal bulk modulus of the fluid
K_f	Effective bulk modulus of the fluid
ℓ	Length of the transmission line
L	Length of the short-tube orifice
L'	Variable defined by Equations (3.13) and (3.14)
m	Variable defined by Equation (4.17)
M_s	Mach number for steady flow through orifice
n	Variable defined by Equation (4.18)
p	Pressure deviation from the mean pressure
p_s	Mean value of pressure

q	Flow rate deviation from the mean flow rate
q_s	Mean flow rate
q_x	$(\partial q/\partial x)$
q_t	$(\partial q/\partial t)$
q_{xx}	$(\partial^2 q/\partial x^2)$
q_{tt}	$(\partial^2 q/\partial t^2)$
$q^{(i)} (i = 0,1,2, \ldots)$	Components of the perturbation solution
r	Coordinate in the radial direction
r_1	Variable defined by Equation (C.13)
r_2	Variable defined by Equation (C.15)
t	Time
u	Fluid velocity in the axial direction
x	Coordinate along the conduit's axis
Z_c	Characteristic impedance of the line
Z_ℓ	Load impedance of the orifice
ZR	A dimensionless ratio (Z_ℓ/Z_c)
ZR1	ZR for a sharp-edged orifice
ZR2	ZR for a short-tube orifice
α	Variable defined by Equation (3.24)
$\alpha 1$	α for a sharp-edged orifice
$\alpha 2$	α for a short-tube orifice
β	Variable defined by Equation (3.25)
$\beta 1$	β for a sharp-edged orifice
$\beta 2$	β for a short-tube orifice
ε	Variable defined by Equation (3.25)
η	Variable defined by Equation (4.21)
θ	Variable defined by Equation (C.14)

λ	Variable defined by Equation (B.6)
μ	Dynamic viscosity of the liquid
ν	Kinematic viscosity of the liquid
ξ	Variable defined by Equation (4.22)
ρ	Equilibrium density of the fluid
ϕ_o	Variable defined by Equation (4.20)
ϕ_1	Variable defined by Equation (4.16)
ϕ_2	Variable defined by Equation (4.26)
ΔP_o	Pressure across the orifice
ω	Circular frequency

CHAPTER I

INTRODUCTION

The study of the dynamic response of fluid transmission lines to time varying input signals has been a subject of absorbing interest to researchers for over a hundred years now. However, some of the most dramatic developments in this area do not date back to more than fifty years. The two primary reasons for such a belated development of the study of fluid transients being the late advent of the digital computer and the not too recently attempted military and space applications of Fluid Control Systems.

An elaborate review of the state of art of fluid transients is beyond the scope of this work. A very lucid and elegant summary of the mathematical models available to date for modeling fluid transients will be found in the paper by Reid (1). Yet another useful review is the paper by Goodson and Leonard (2).

This work is concerned primarily with the frequency response of a fluid transmission line terminated by an orifice with a nonlinear pressure flow characteristic. An important example is the case of a fluid control system in which a fluid line is terminated by a control valve. In the frequency response analysis of such a system it is customary to linearize the orifice-flow equation before incorporating it as a boundary condition for the fluid line. Such a procedure proves satisfactory for signals with a small amplitude. For finite amplitude signals, however,

the nonlinearity of the orifice's pressure flow characteristic leads to the generation of higher harmonics of the line at the orifice (Figure 1). These higher harmonics can endanger the stability of a system adjoining the line.

It should be noted at this stage that by the name "finite amplitude signal" reference is made to those signals for which the nonlinearity of the orifice characteristic cannot be ignored. It is assumed, however, that these signals do not invalidate the linearization and the subsequent perturbation of the Navier-Stokes equations.

Recently Strunk (3) has reported a perturbation solution for the frequency response of a fluid line with a nonlinear boundary condition. His study has revealed excellent agreement between the perturbation solution and the solution obtained through the finite difference method. The derivation of closed-form solutions for both the amplitude and phase response of the fundamental as well as the higher harmonics of the line through the application of the perturbation method is the highlight of Strunk's work.

The basic orifice-flow model employed by Strunk (3), however, neglects the inertance effect of the orifice, which may become important at very high frequencies.

Subsequent to the publication of the paper by Strunk (3), several studies have been carried out by teams of researchers engaged in diverse fields of application of fluid mechanics. Notable among these studies are the papers by Funk et al. (4), Lahey and Shiralkar (5), and Yellin and Peskin (6). The mathematical models presented by these authors account for not only the nonlinear pressure flow characteristic of the orifice but also its inertance effect.

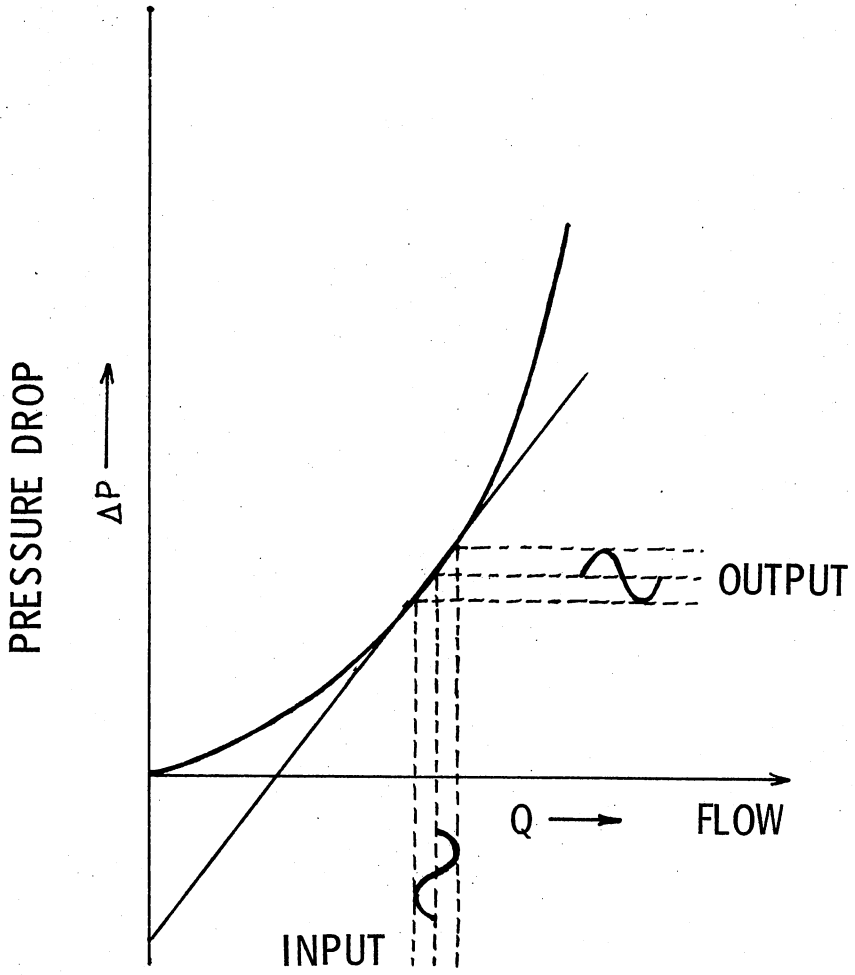

Figure 1. Pressure Response of an Orifice to a Sinusoidal Flow Input

In this work consideration is limited to the case of a nonviscous fluid line. Based on the orifice-flow model, due to Funk et al. (Chapter II), the author has derived a modified boundary condition, in terms of flow rate, for the case of a fluid line terminated by a nonlinear orifice. The details of formulation of the boundary value problem are presented in Chapter III. In Chapter IV closed-form perturbation solutions for the amplitude and phase response of the fundamental and the second harmonic, including the inertance effect of the orifice, are presented.

Identification of the dimensionless parameters of the system and the subsequent nondimensionalization of the expressions for the amplitude and phase response of the fundamental and the percentage second harmonic distortion is presented in Chapter V. In this same chapter it is also shown that with the inclusion of the inertance effect of the orifice a new dimensionless number comes into the picture. Equations defining this dimensionless number for the case of a sharp-edged orifice as well as a short-tube orifice are presented.

In Chapter VI the results of numerical computations of the frequency response and the percentage second harmonic distortion are discussed at length. Chapter VII presents a brief review of this work together with the major conclusions reached through this study regarding the influence of the inertance effect of the orifice on the system's frequency response at high frequencies of operation. A few recommendations for future extension of this work are included.

CHAPTER II

TRANSIENT RESPONSE OF AN ORIFICE: A LITERATURE SURVEY

The basic equation governing the steady incompressible flow of fluid across a circular orifice is

$$q_o = C_d A_o \sqrt{\frac{2(\Delta p_o)}{\rho}}$$

i.e.,

$$\Delta p_o = K' q_o^2 \tag{2.1}$$

where

$$K' = \rho/2(C_d A_o)^2; \tag{2.2}$$

q_o = total flow through the orifice;

p_o = pressure drop across the orifice.

Equation (2.1) is generally referred to as the steady-state pressure-flow characteristic of an orifice. In most engineering applications of orifice meters, wherein the flow is unsteady, it is generally assumed that an orifice closely follows its steady-state characteristic during transient operation. This implies that the flow conditions stabilize instantaneously from one steady-state value to another steady-state value. Owing to the high value of the speed of sound in an incompressible fluid, such an assumption of quasi-steady behavior proves satisfactory for most flow cases wherein the amplitude of the disturbance is small and frequencies of operation are low.

For large amplitude unsteady flows, however, the coefficient of discharge C_d could become sensitive to the variations in the Reynolds number. To date the variation of C_d for transient flow across an orifice is unknown.

Secondly, for flow measurements in a system with rapidly occurring transients, if a sharp-edged orifice is used in conjunction with a high frequency pressure transducer, the recorded measurements must in general be corrected for inertial effects of the orifice as well as the pressure transducer and the associated electronics.

The inertial or the inertance effect of an orifice leads to a pressure drop across the orifice which is in excess of that given by Equation (2.1). To date several teams of researchers engaged in such diverse fields of application of fluid mechanics as hydraulics, biomedical engineering, etc. have reported closed form, analytical models for pulsatile flow across an orifice which account not only for its nonlinear pressure-flow characteristic, but also its inertance effect. A brief review of these models is presented below.

Funk, Wood and Chao's Model (4)

Assuming potential flow and considering the flow field to the left of the orifice as "flow into a sink" and the flow field to the right as "flow out of a source," these authors have reported the following models for the transient response of an orifice.

(a) Sharp-edged orifice:

$$p_1 - p_2 = \frac{\rho}{\sqrt{\frac{C_d A_o \pi}{2}}} \cdot \left[\frac{dq}{dt}\right] + \frac{\rho q^2}{2(C_d A_o)^2} \qquad (2.3)$$

(b) Short-tube orifice:

$$p_1 - p_2 = \left[\frac{\rho}{\sqrt{\frac{C_d A_o \pi}{2}}} + \frac{\rho L}{A_o}\right] \frac{dq}{dt} + \left[\frac{\rho}{2(C_d A_o)^2} + \frac{\rho f L}{2D_o A_o^2}\right] q^2 \quad (2.4)$$

Their experimental results have shown excellent agreement with the theory.

Lahey and Shiralkar's Model (5)

The work reported by these authors concerns the response characteristic of sharp-edged orifices for transient flow measurements. The need for simulating the loss-of-coolant or loss-of-pump accident in a water-cooled nuclear reactor has been cited as a typical application wherein the transient response of an orifice is of major importance.

A solution for the inertial correction involved in the measurement of flow during an exponential pressure decay across the orifice has been reported.

Yellin and Peskin's Model (6)

These authors have investigated the problem of steady-state oscillatory blood flow across heart valves by developing the following orifice flow model:

$$p_1 - p_2 = K_1 \frac{dq}{dt} \pm K_2 q^2 \quad \begin{cases} +: q>0 \\ -: q<0 \end{cases} \quad (2.5)$$

where

$$K_1 = \frac{\rho L C_\delta^2}{A_o} \quad (2.6)$$

$$L = A_o \int_{x_1}^{x_c} dx/A(x)$$

x_c = location of the vena contracta

$C_\delta = p_1 - p_2/p_1 - p_c$

$\Delta p_o = p_1 - p_2$

p_c = pressure at vena contracta

$$K_2 = \frac{\rho}{2A_o^2}\left(\frac{C_\delta}{C_c}\right)^2 \left[1 - \left(\frac{A_o}{A_\ell}\cdot C_c\right)^2\right] \tag{2.7}$$

The experimental results of Yellin and Peskin (6) encompass the physiological range: large amplitude pulsations of low frequency (less than 200/min).

In this thesis the orifice model due to Funk, Wood and Chao (4) has been used to derive a modified boundary condition for a fluid line terminated by a nonlinear inertive orifice. The details of the formulation of the boundary value problem are presented in the following chapter.

CHAPTER III

FORMULATION OF THE BOUNDARY VALUE PROBLEM

In the following analysis cylindrical coordinates have been employed to describe the phenomenon of fluid flow through a circular wave guide of finite length ℓ. The x-axis is identified with the center line of the conduit and r is a coordinate in the radial direction.

The Basic Differential Equations

The basic differential equations governing the propagation of small amplitude disturbances in a liquid filled tube of circular cross section are (7):

(a) Equation of Motion: x-Direction:

$$\rho \frac{\partial u}{\partial t} = - \frac{\partial p}{\partial x} + \mu \cdot [\frac{\partial^2 u}{\partial r^2} + \frac{1}{r} \cdot \frac{\partial u}{\partial r}] \tag{3.1}$$

i.e.,

$$\frac{\partial u}{\partial t} = - \frac{1}{\rho} \cdot \frac{\partial p}{\partial x} + \nu(\frac{1}{r}) \frac{\partial}{\partial r} [r \cdot \frac{\partial u}{\partial r}] \tag{3.2}$$

(b) Continuity Equation:

$$\frac{\partial \rho}{\partial t} + \rho \frac{\partial v}{\partial r} + \rho \frac{v}{r} + \rho \frac{\partial u}{\partial x} = 0 \tag{3.3}$$

(c) Equation of State for a Liquid:

$$\frac{\partial \rho}{\rho} = \frac{\partial p}{K_f} \tag{3.4}$$

where $u(x,r,t)$ and $v(x,r,t)$ are the deviations of the components of the velocity vector in the x and r directions from their respective steady-state values. Similarly, $p(x,r,t)$ represents the deviation of pressure from its mean steady-state value.

Assumptions

The above mentioned equations apply when the following assumptions are true:

1. The elasticity of the pipe walls is neglected when compared with the compressibility of the liquid.

2. The variations in the fluid's temperature are small so that viscosity is considered to remain constant. Stipulation of negligible thermal effects also eliminates the energy equation as one of the describing equations.

3. The variations of all dependent variables in the circumferential direction are negligible due to rotational symmetry.

4. Small amplitude laminar disturbances are assumed. This implies that the Reynolds' number is less than 2000 and that the pressure gradients are small enough so that wave shape changes due to changes in the speed of sound are negligible.

5. The velocity component u is $>>$ v. The equation of motion in the radial direction is therefore neglected. Neglect of this equation implies that the pressure is constant across the cross section of the tube and becomes a function only of x and t. That is, the disturbance is a plane wave, with the pressure $p(x,t)$ and the density $\rho(x,t)$ remaining uniform across the pipe.

6. The nonlinear convective acceleration terms on the left hand side of the equation of motion are small when compared with the local acceleration term $\frac{\partial u}{\partial t}$.

7. The only important viscous terms on the right hand side of Equation (3.1) are $\frac{\partial^2 u}{\partial r^2}$ and $\frac{1}{r} \cdot \frac{\partial u}{\partial r}$.

8. Due to the high value of the bulk modulus of a liquid, the terms $v \cdot \frac{\partial \rho}{\partial r}$ and $u \cdot \frac{\partial \rho}{\partial x}$ are considered small and neglected in writing the equation of continuity.

9. The fluid velocity u is less than the sonic velocity c; this implies that the flow is subsonic.

10. The conduit has a circular cross section which is constant throughout its length.

The temporal variation of fluid density in Equation (3.3) may be eliminated by combining Equations (3.3) and (3.4). Thus Equations (3.1) to (3.4) reduce to the following two partial differential equations:

$$\frac{\partial u}{\partial t} = - \frac{1}{\rho} \cdot \frac{\partial p}{\partial x} + \nu \left(\frac{1}{r}\right) \cdot \frac{\partial}{\partial r} \left[r \cdot \frac{\partial u}{\partial r}\right] \tag{3.5}$$

and

$$\frac{1}{K_f} \cdot \frac{\partial p}{\partial t} + \frac{\partial v}{\partial r} + \frac{v}{r} + \frac{\partial u}{\partial x} = 0 \tag{3.6}$$

This work is restricted to the consideration of a nonviscous fluid line only. Hence, the viscous terms may be omitted and Equation (3.5) rewritten as

$$\frac{\partial u}{\partial t} = - \frac{1}{\rho} \cdot \frac{\partial p}{\partial x} \tag{3.7}$$

Define $\bar{u}$ to be the average fluid velocity and $\bar{p}$ to be the average pressure across a cross section. By multiplying Equation (3.6) by $2\pi r$ and integrating over the cross section, Equation (3.6) becomes

$$\frac{1}{K_f} \cdot \frac{\partial \bar{p}}{\partial t} = - \frac{\partial \bar{u}}{\partial x} \tag{3.8}$$

From assumptions 3 and 5, $p = \bar{p}$. Next, defining the flow rate $q(x,t)$ by the relation

$$q(x,t) = (\pi a^2) \cdot \bar{u} \tag{3.9}$$

Equation (3.8) can be expressed as

$$\frac{\partial p}{\partial t} = - \left(\frac{K_f}{\pi a^2}\right) \cdot \frac{\partial q}{\partial x} \tag{3.10}$$

Combining Equations (3.7) and (3.10) the spatial domain model for a non-viscous fluid line reduces to the following one-dimensional wave equation:

$$\frac{\partial^2 q}{\partial t^2} - c^2 \frac{\partial^2 q}{\partial x^2} = 0 \tag{3.11}$$

where

$$c = (K_f/\rho)^{1/2}$$

$$K_f = K_3/(1 + (D/b) \cdot (K_3/E))$$

and

c = speed of sound in fluid;

K_f = the effective bulk modulus of the fluid;

K_3 = isothermal bulk modulus of the fluid;

D = internal diameter of the line;

b = wall thickness of the conduit;

E = modulus of elasticity of the material of the conduit;

ρ = fluid density.

Boundary Condition

The orifice model due to Funk et al. (4) may be used to derive a boundary condition for the nonviscous line in terms of the flow rate q. This model may be expressed in the form

$$\Delta p_o = L' \dot{q}_o + K' q_o^2 \tag{3.12}$$

where

q_o = instantaneous total flow rate through the orifice;

Δp_o = instantaneous pressure drop across the orifice.

For a sharp-edged orifice,

$$L' = \rho/\sqrt{\left(\frac{C_d A_o \pi}{2}\right)} \tag{3.13}$$

$$K' = \rho/2(C_d A_o)^2$$

and for orifices with significant axial dimension (sometimes referred to as short-tube orifices),

$$L' = \rho/\sqrt{\left(\frac{C_d A_o \pi}{2}\right)} + \rho L/A_o \tag{3.14}$$

$$K' = \rho/2(C_d A_o)^2 + \rho f L/[A_o^2 (2D_o)]$$

Assume that the flow is discharging to the atmosphere, and let the deviations in the flow and pressure from their respective mean values (q_s and p_s) be

$$q = q_o - q_s \tag{3.15}$$

$$p = \Delta p_o - p_s$$

Then,

$$\begin{aligned} \Delta p_o &= p_{upstream} - p_{downstream} \\ &= p_{upstream} \\ &= \Delta p_o . \end{aligned} \tag{3.16}$$

Rewriting Equation (3.12),

$$\Delta p_o = L' \cdot \dot{q}_o + K' q_o^2 \tag{3.17}$$

Substituting for Δp_o and q_o from Equation (3.15) into Equation (3.17), we have

$$p + p_s = L' \frac{d}{dt} [q + q_s] + K' [q + q_s]^2 \tag{3.18}$$

The mean value of pressure p_s associated with steady flow case is thus

$$p_s = K' q_s^2 \tag{3.19}$$

Substituting for pressure p_s in Equation (3.18), we have

$$p = L' \dot{q} + K' q^2 + 2K' q q_s \tag{3.20}$$

Differentiating Equation (3.20) with respect to time, we have

$$\dot{p} = L' \ddot{q} + 2K' [q + q_s] \dot{q} \tag{3.21}$$

Eliminating $\dot{p}$ by using Equation (3.10), the boundary condition for a nonviscous fluid line terminated by an orifice may be expressed in terms of flow rate as

$$-\left(\frac{K_f}{\pi a^2}\right) q_x = L' \ddot{q} + 2K' [q + q_s] \dot{q}$$

i.e.,

$$q_x + \alpha \dot{q} + \beta \ddot{q} = -\varepsilon q \dot{q} \tag{3.22}$$

where

$$\varepsilon = 2K' (\pi a^2)/K_f \tag{3.23}$$

$$\alpha = (2K' q_s) \cdot (\pi a^2)/K_f = \varepsilon q_s \tag{3.24}$$

$$\beta = L' \cdot (\pi a^2)/K_f \tag{3.25}$$

Equations (3.20) and (3.-2) are valid for $q_s > -q$.

For the frequency response analysis of a nonviscous line terminated by a nonlinear orifice, the boundary value problem thus consists of solving Equation (3.11) subject to the boundary conditions.

At $x = 0$,

$$q = A \cdot \sin(\omega t) \tag{3.26}$$

and at $x = \ell$,

$$q_x = \alpha q_t + \beta q_{tt} = -\varepsilon q q_t .$$

CHAPTER IV

THE PERTURBATION SOLUTION: NONVISCOUS LINE

The boundary value problem as formulated in Chapter III consists in solving the elementary wave equation

$$q_{tt} - c^2 q_{xx} = 0 \tag{4.1}$$

subject to the boundary conditions

$$q = A \sin(\omega t), \text{ at } x = 0$$

$$q_x + \alpha q_t + \beta q_{tt} = -\varepsilon q q_t, \text{ at } x = \ell. \tag{4.2}$$

Equation (4.1) is a linear second order partial differential equation; as such it requires two initial conditions and two boundary conditions for a complete solution. However, if the boundary conditions have acted long enough, the transient effects created by the initial conditions are of no consequence. The solution for frequency response may thus be obtained by solving Equation (4.1) subjected to boundary conditions (Equation (4.2)) alone.

The nonlinearity associated with the second boundary condition presents considerable difficulty in obtaining an exact closed from solution for $q(x, t)$. Following Strunk (3) an approximate solution to the boundary value problem can be obtained by applying the perturbation method. Assuming that the perturbed solution is analytic with respect to the parameter ε, the total solution is sought in the form of a power

series ε, given by:

$$q(x, t) = \sum_{i=0}^{\infty} \varepsilon^i q^{(i)}(x, t). \tag{4.3}$$

For ε sufficiently small, a good approximation is obtained by considering only the first two or three terms of the perturbed solution.

Substituting Equation (4.3) in Equations (4.1) and (4.2), one obtains an infinite set of linear partial differential equations subjected to linear boundary conditions (Appendix A). The first three sets of system equations are:

For $O(\varepsilon = 0)$,

$$q_{tt}^{(o)} - c^2 q_{xx}^{(o)} = 0$$

$$q^{(o)} = A \cdot \sin(\omega t), \text{ at } x = 0$$

$$q_x^{(o)} + \alpha q_t^{(o)} + \beta q_{tt}^{(o)} = 0, \text{ at } x = \ell. \tag{4.4}$$

For $O(\varepsilon)$,

$$q_{tt}^{(1)} - c^2 q_{xx}^{(1)} = 0$$

$$q^{(1)} = 0, \text{ at } x = 0$$

$$q_x^{(1)} + \alpha q_t^{(1)} + \beta q_{tt}^{(1)} = -q^{(o)} q_t^{(o)}, \text{ at } x = \ell. \tag{4.5}$$

For $O(\varepsilon^2)$,

$$q_{tt}^{(2)} - c^2 q_{xx}^{(2)} = 0$$

$$q^{(2)} = 0, \text{ at } x = 0. \tag{4.6}$$

And at $x = \ell$,

$$q_x^{(2)} + \alpha q_t^{(2)} + \beta q_{tt}^{(2)} = -[q^{(o)} q_t^{(1)} + q^{(1)} q_t^{(o)}]$$

where the notation used is

$$q_x = \frac{\partial q}{\partial x},\ q_t = \frac{\partial q}{\partial t},\ q_{xx} = \frac{\partial^2 q}{\partial x^2},\ q_{tt} = \frac{\partial^2 q}{\partial t^2}\ .$$

This system of linear equations may be solved successively for the terms $q^{(i)}(x, t)$, $(i = 0, 1, 2, 3, \ldots)$ of the assumed solution (4.3) by starting with the first set (4.4). The set (4.4) is the linearized form of the original Equation (4.1) and the boundary conditions (4.2).

The solution for $q^{(o)}(x, t)$ at $x = \ell$ becomes the forcing function for the set (4.5) and likewise each successive solution is influenced by the previous solutions. For this reason, the set (4.4) is termed the generating system, and its solution, $q^{(o)}(x, t)$, is called the generating solution.

The generating system was solved by the method of separation of variables, using a complex exponential representation for the boundary conditions (Appendices B and C). The solution is

$$q^{(o)}(x, t) = A\left[\left\langle \cos(\lambda x) + \frac{2r_2 \sin(2\lambda\ell-\theta)\cdot\sin(\lambda x)}{1 + 2r_2 \cos(2\lambda\ell-\theta) + r_2^2}\right\rangle \sin(\omega t)\right.$$

$$\left. + \left\langle \frac{(r_2^2 - 1)\sin(\lambda x)}{1 + 2r_2 \cos(2\lambda\ell-\theta) + r_2^2}\right\rangle \cos(\omega t)\right] \qquad (4.7)$$

where

$$\lambda = \omega/c \text{ (Appendix B)}; \qquad (4.8)$$

$$r_2 = r_1/[(1 + \alpha c)^2 + (\beta c\omega)^2] \qquad (4.9)$$

$$r_1 = \left[\{1 - (\alpha c)^2 - (\beta c\omega)^2\}^2 + 4(\beta c\omega)^2\right]^{1/2} \qquad (4.10)$$

$$\theta = \tan^{-1}\left[-2\beta c\omega/\{1 - (\alpha c)^2 - (\beta c\omega)^2\}\right] \qquad (4.11)$$

When the inertance effect of the orifice is neglected ($\beta = 0$), Equation (4.7) reduces to (Appendix D):

$$q^{(o)}(x, t) = A\left[\left\langle \cos(\lambda x) + \frac{(1-\alpha^2c^2)\sin(\lambda\ell)\cos(\lambda\ell)}{\cos^2(\lambda\ell) + \alpha^2c^2\cdot\sin^2(\lambda\ell)} \sin(\lambda x)\right\rangle \right.$$

$$\left. \sin(\omega t) - \left\langle \frac{(\alpha c)\sin(\lambda x)}{\cos^2(\lambda\ell) + \alpha^2c^2\sin^2(\lambda\ell)} \right\rangle \cos(\omega t)\right]. \tag{4.12}$$

Equation (4.12) is identical to Equation (23) reported by Strunk (3).

Next, considering Equation (4.7) again, the solution at $x = \ell$ becomes (Appendix E):

$$q^{(o)}(\ell, t) = A_1\cdot\sin(\omega t + \phi_1) \tag{4.13}$$

where

$$A_1 = A(B_1) \tag{4.14}$$

$$B_1 = \frac{\sqrt{m^2 + n^2}}{[1 + 2r_2\cos(2\lambda\ell-\theta) + r_2^2]} \tag{4.15}$$

$$\phi_1 = \tan^{-1}[n/m] \tag{4.16}$$

$$m = B\cdot\sin(2\lambda\ell + \phi_o) \tag{4.17}$$

$$n = (r_2^2 - 1)\cdot\sin(\lambda\ell) \tag{4.18}$$

$$B = \sqrt{\eta^2 + \xi^2} \tag{4.19}$$

$$\phi_o = \tan^{-1}[\eta/\xi] \tag{4.20}$$

$$\eta = 1 + r_2^2 + 2r_2\cos(\theta) \tag{4.21}$$

$$\xi = 2r_2\cdot\sin(\theta) \tag{4.22}$$

Notice Equation (4.13) is functionally of the same form as Equation (24) reported by Strunk (3). The parameters B_1 and ϕ_1, however, now assume a new definition in the light of the inertance effect of the orifice at $x = \ell$.

Next, from Equation (4.13), we have

$$q_t^{(o)}(\ell, t) = (\omega A_1)\cdot\cos(\omega t + \phi_1)$$

$$q^{(o)}(\ell, t)\, q_t^{(o)}(\ell, t) = \omega A_1^2\cdot\sin(\omega t + \phi_1)\cdot\cos(\omega t + \phi_1)$$

$$= \frac{1}{2}\,\omega A_1^2\cdot\sin(2\omega t + 2\phi_1) \qquad (4.23)$$

Equation (4.23) is the forcing function for the set (4.5). By once again using the method of separation of variables, the solution for set (4.5) becomes (Appendix F):

$$q^{(1)}(x, t) = -\frac{1}{4}\, c\, A_1^2\, (B_2)\cdot\sin(2\lambda x)\cdot\sin(2\omega t + 2\phi_1 + \phi_2) \qquad (4.24)$$

where

$$B_2 = [\{\cos(2\lambda\ell) - 2\beta c\omega\cdot\sin(2\lambda\ell)\}^2 + \{\alpha c\cdot\sin(2\lambda\ell)\}^2]^{-1/2} \qquad (4.25)$$

$$\phi_2 = \tan^{-1}[-\alpha c/\{\cot(2\lambda\ell) - 2(\beta c\omega)\}] \qquad (4.26)$$

Equation (4.24) is again functionally of the same form as Equation (26) reported by Strunk (3); the parameters A_1, B_2, ϕ_1, and ϕ_2 now assume a new definition in the light of the inertance effect of the orifice at $x = \ell$. Notice that the solution $q^{(1)}(x, t)$ given by Equation (4.24) constitutes a second harmonic component of the total solution $q(x, t)$. By continuing this process, additional harmonic components will be obtained, and thus the approximate solution improved. Strunk (3) has found, however, that the amplitudes of the higher harmonics are less than one percent of the amplitude of the fundamental. Hence only the first two terms in Equation (4.3) have been included in the results presented in this chapter.

CHAPTER V

NONDIMENSIONAL FREQUENCY RESPONSE AND PERCENTAGE SECOND HARMONIC DISTORTION

In this chapter expressions for the frequency response of a nonviscous fluid line and the percentage second harmonic distortion of the input signal resulting from the nonlinearity of the boundary condition at $x = \ell$ are derived. These expressions will be subsequently shown to be functions of the following nondimensional ratios:

XL = x/ℓ, axial position number;

FN = $\omega\ell/c$, frequency number;

$M_s = q_s/(A_o c)$, mach number of steady flow through the orifice;

AQ = A/q_s, ratio of input flow amplitude to mean flow amplitude;

AR = $\pi a^2/A_o$, ratio of line's cross sectional area to orifice area;

BCP1 = $(AR)(M_s)$, a boundary condition parameter;

BCP21 = $(\beta 1)(c\omega)$, a boundary condition parameter referred to a sharp-edge orifice ($\beta 1$ is defined below);

BCP22 = $(\beta 2)(c\omega)$, a boundary condition parameter referred to a short-tube orifice ($\beta 2$ is defined below).

From Equation (3.25),

$$\beta = L' \cdot (\pi a^2)/K_f.$$

Hence, using Equations (3.13) and (3.14), one may write for a sharp-edged orifice,

$$\beta 1 = (\rho/\sqrt{\frac{C_d A_o \pi}{2}}) \cdot (\frac{\pi a^2}{K_f})$$

and for a short-tube orifice,

$$\beta 2 = (\rho/\sqrt{\frac{C_d A_o \pi}{2}} + \rho L/A_o) \cdot (\frac{\pi a^2}{K_f}).$$

It may be readily verified that both BCP21 and BCP22 are nondimensional parameters.

Next, consider the dimensionless ratios,

$$ZR1 = (\alpha 1)c = [1/(C_d)^2] \cdot BCP1;$$

$$ZR2 = (\alpha 2)c = [1/(C_d)^2 + f(L/D_o)] \cdot BCP1.$$

From Equation (3.24),

$$\alpha = (2K' q_s) \cdot (\pi a^2)/(K_f).$$

Hence, using Equations (3.13) and (3.14), one may write for a sharp-edged orifice,

$$\alpha 1 = (\rho/(C_d A_o)^2) \cdot q_s \cdot (\pi a^2)/(K_f)$$

and for a short-tube orifice,

$$\alpha 2 = [\rho/(C_d A_o)^2 + \rho f L/(D_o A_o^2)] \cdot q_s \cdot \pi a^2/(K_f).$$

It may be noted at this stage that Equation (7) reported by Strunk (3) is incorrect. The correct version of this equation is Equation (2.1). This discrepancy in the form of equations affects the definition of the parameter K' and consequently causes a 2 to appear erroneously in Strunk's (3) definition of ZR. Expressions for ZR1 and ZR2 are derived in Appendix G.

The inclusion of the inertance effect of the orifice in the analysis brings into consideration an additional dimensionless ratio defined by BCP21 (or BCP22).

Amplitude Ratio: Fundamental

Next, consider Equation (4.7) which has been reproduced below,

$$q^{(o)}(x, t) = A\left[\left\langle \cos(\lambda x) + \frac{2r_2 \cdot \sin(2\lambda\ell-\theta)}{1+2r_2\cos(2\lambda\ell-\theta)+r_2^2}\sin(\lambda x)\right\rangle \sin(\omega t) + \left\langle \frac{(r_2^2-1)\cdot\sin(\lambda x)}{1+2r_2\cos(2\lambda\ell-\theta)+r_2^2}\right\rangle \cdot \cos(\omega t)\right].$$

One may rewrite this equation as,

$$q^{(o)}(x, t) = A\cdot(B_3)\cdot[\{b(x)\}\sin(\omega t) + \{a(x)\}\cos(\omega t)] \quad (5.1)$$

where

$$B_3 = 1/[1 + 2r_2\cos(2\lambda\ell-\theta) + r_2^2] \quad (5.2)$$

$$b(x) = [\{1 + 2r_2\cos(2\lambda\ell-\theta) + r_2^2\}\cos(\lambda x) + 2r_2\cdot\sin(2\lambda\ell-\theta)\cdot\sin(\lambda x)] \quad (5.3)$$

$$a(x) = [\{r_2^2 - 1\}\cdot\sin(\lambda x)]. \quad (5.4)$$

From Equation (5.1),

$$q^{(o)}(x, t) = A\cdot(B_3)\cdot c(x)\cdot\sin(\omega t + \phi(x)) \quad (5.5)$$

where

$$c(x) = [a^2(x) + b^2(x)]^{1/2} \quad (5.6)$$

and

$$\phi(x) = \tan^{-1}[a(x)/b(x)]. \quad (5.7)$$

Hence, the amplitude ratio for the generating solution is:

$$\frac{|q^{(o)}(x, t)|}{A} = B_3 \cdot c(x) \tag{5.8}$$

Nondimensional plots of frequency response of a nonviscous line given by Equation (5.8) are presented in Chapter VI.

Before proceeding to the consideration of the second harmonic distortion, it is important to see how each term appearing in Equation (5.8) can be expressed in terms of nondimensional ratios defined at the beginning of this chapter.

From Equation (4.10),

$$r_1 = [\{1 - (\alpha c)^2 - (\beta c \omega)^2\}^2 + 4(\beta c \omega)^2]^{1/2}$$

Thus, for the case of a sharp-edged orifice:

$$r_1 = [\{1 - (ZR1)^2 - (BCP21)^2\}^2 + 4(BCP21)^2]^{1/2}. \tag{5.9}$$

Next, from Equation (4.9),

$$r_2 = r_1/\{(1 + \alpha c)^2 + (\beta c \omega)^2\}$$

i.e.,

$$r_2 = r_1/\{(1 + ZR1)^2 + (BCP21)^2\}. \tag{5.10}$$

Also from Equation (4.11),

$$\theta = \tan^{-1}[-2\beta c \omega/\{1 - (\alpha c)^2 - (\beta c \omega)^2\}]$$

i.e.,

$$\theta = \tan^{-1}[-2(BCP21)/\{1 - (ZR1)^2 - (BCP21)^2\}] \tag{5.11}$$

Next, from Equation (4.8),

$$2\lambda \ell = 2(\omega/c)\ell = 2(FN) \tag{5.12}$$

and

$$\lambda x = \frac{\omega x}{c} = \frac{\omega \ell}{c} \cdot \frac{x}{\ell} = (FN) \cdot (XL). \tag{5.13}$$

Thus, the arguments of the circular functions appearing in Equations (5.3) and (5.4) may be expressed in terms of the dimensionless ratios FN, XL etc. Equation (5.8) can also be rewritten as a nondimensional equation.

Percentage Second Harmonic Distortion

Next, consider the second harmonic distortion. From Equation (4.24)

$$q^{(1)}(x, t) = -\frac{1}{4} \cdot c\, A_1^2\, (B_2) \cdot \sin(2\lambda x) \cdot \sin(2\omega t + 2\phi_1 + \phi_2)$$

$$\therefore\ |\varepsilon q^{(1)}(x, t)| = \varepsilon \cdot \{\frac{1}{4} \cdot c\, A_1^2\, (B_2) \cdot \sin(2\lambda x)\} \qquad (5.14)$$

Hence, from Equation (5.8) and Equation (5.14) the harmonic distortion due to the second harmonic is obtained as:

$$\frac{|\varepsilon q^{(1)}(x, t)|}{|\, q^{(o)}(x, t)|} = \frac{\varepsilon \cdot \frac{1}{4} \cdot c\, A_1^2 \cdot (B_2) \cdot \sin(2\lambda x)}{A \cdot (B_3) \cdot c(x)} \qquad (5.15)$$

From Equation (4.14),

$$A_1 = A(B_1)$$

and from Equation (3.24),

$$\varepsilon = \frac{(\alpha 1)}{q_s}$$

(for a sharp-edged orifice).

Substituting for A_1 and ε in Equation (5.15),

$$\frac{|\varepsilon \cdot q^{(1)}(x, t)|}{|\, q^{(o)}(x, t)\,|} = \frac{1}{4} \cdot (\frac{A}{q_s}) \cdot (ZR1) \cdot (\frac{B_1^2\, B_2}{B_3}) \cdot \frac{\sin(2\lambda x)}{c(x)} \,. \qquad (5.16)$$

Hence, the percentage second harmonic distortion is given by,

$$\frac{|\varepsilon\, q^{(1)}(x, t)|}{|\, q^{(o)}(x, t)\,|} = (25.0) \cdot (\frac{A}{q_s}) \cdot (ZR1) \cdot (\frac{B_1^2\, B_2}{B_3}) \cdot \frac{\sin(2\lambda x)}{c(x)} \,. \qquad (5.17)$$

In the above equation, $\sin(2\lambda x) = \sin(2 \cdot FN \cdot XL)$.

The product $(B_3 \cdot c(x))$ appearing in Equation (5.17) above constitutes Equation (5.8) which has already been shown to be amenable to nondimensionalisation. From Equation (4.25),

$$B_2 = [\{\cos(2\lambda\ell) - 2(\beta c\omega)\sin(2\lambda\ell)\}^2 + \{\alpha c \cdot \sin(2\lambda\ell)\}^2]^{-1/2}$$

Therefore, for the case of a line terminated by a sharp-edged orifice,

$$B_2 = [\{\cos(2 \cdot FN) - 2(BCP21) \cdot \sin(2 \cdot FN)\}^2 + \{(ZR1) \cdot \sin(2 \cdot FN)\}^2]^{-1/2} \quad (5.18)$$

From Equations (4.15) and (5.2),

$$B_1^2 = (m^2 + n^2) \cdot B_3^2 \quad (5.19)$$

From Equations (4.17, 4.19, 4.20, 4.21, and 4.22),

$$m^2 = [\{1 + r_2^2 + 2r_2 \cos(\theta)\}^2 + \{2r_2 \cdot \sin(\theta)\}^2] \sin^2(\lambda\ell + \phi_o) \quad (5.20)$$

where from Equations (4.20, 4.21 and 4.22),

$$\phi_o = \tan^{-1}\left[\frac{1 + r_2^2 + 2r_2 \cos(\theta)}{2r_2 \cdot \sin(\theta)}\right] . \quad (5.21)$$

From Equation (4.18)

$$n^2 = (r_2^2 - 1) \cdot \sin^2(\lambda\ell). \quad (5.22)$$

It has already been shown that the terms r_1, r_2, $\lambda\ell$, λx, θ etc. can be expressed as functions of nondimensional ratios FN, XL, BCP1 etc. Thus B_1^2 given by Equation (5.19) may be readily nondimensionalized. This implies that the percentage second harmonic distortion given by

Equation (5.17) can also be expressed as a function of nondimensional ratios, defined at the beginning of this chapter.

The listing of the computer programs (Appendix H) may be referred to for the numerical computation of nondimensional frequency response and the percentage second harmonic distortion.

CHAPTER VI

DISCUSSION OF RESULTS

The nondimensional plots presented in this chapter refer to the variation of (a) the amplitude ratio of the fundamental Equation (5.8), and (b) the percentage second harmonic distortion Equation (5.17) as functions of the frequency number FN and the axial position number XL for fixed values of the boundary condition parameters BCP1 and BCP21. The parameter BCP1 has been varied from a value of 0.01 to 1.0, while BCP21 has been considered for the range 0.0 to 0.65. Sample values for BCP21 for a typical line-orifice system have been tabulated in Table I. Plots with BCP21 = 0.0 correspond to the case wherein the inertance effect of the orifice has been neglected. These plots are identical to those presented by Strunk (3). Strunk's results are, however, in error due to his usage of an incorrect form of the orifice-flow equation. The error resulting from such an incorrect usage, however, is local in nature and remains restricted to the definition of the nondimensional parameter ZR1. Figures 2 and 3 demonstrate how, for a given FN, BCP1 and BCP21, the amplitude ratio of the fundamental and the percentage second harmonic distortion are affected by the incorrect definition of ZR1 at different locations along the line. In this work the results obtained by Strunk (3) have been corrected and reproduced for the specific purpose of comparison with the author's results.

TABLE I

SAMPLE VALUES FOR BCP21 AND BCP22 FOR
A TYPICAL LINE ORIFICE SYSTEM

Fluid density = 3×10^{-5} lb $sec^2/ft\text{-}in.^4$ Ratio $K_f/E = 0.01$

Bulk modulus of fluid = 3×10^5 psi Coefficient of discharge = 0.6

Inner diameter of line = 1.0 in. Diameter of orifice = 0.25 in.

Wall thickness of line = 0.0625 in. Thickness of orifice = 0.125 in.

w(Rad/Sec)	Frequency (Cyc/sec)	BCP21	BCP22
0.0	0.00	0.0	0.0
100.0	15.92	0.00554	0.00857
500.0	79.58	0.02768	0.04284
1000.0	159.16	0.05536	0.08569
1500.0	238.73	0.08305	0.12853
2000.0	318.31	0.11073	0.17137
2500.0	397.89	0.13841	0.21422
3000.0	477.47	0.16609	0.25706
3500.0	557.04	0.19377	0.29991
4000.0	636.62	0.22145	0.34275
5000.0	795.78	0.27682	0.42844
6000.0	954.93	0.33218	0.51413
7000.0	1114.09	0.38755	0.59981
8000.0	1273.24	0.44291	0.68550
9000.0	1432.40	0.49827	0.77119
10000.0	1591.55	0.55364	0.85688

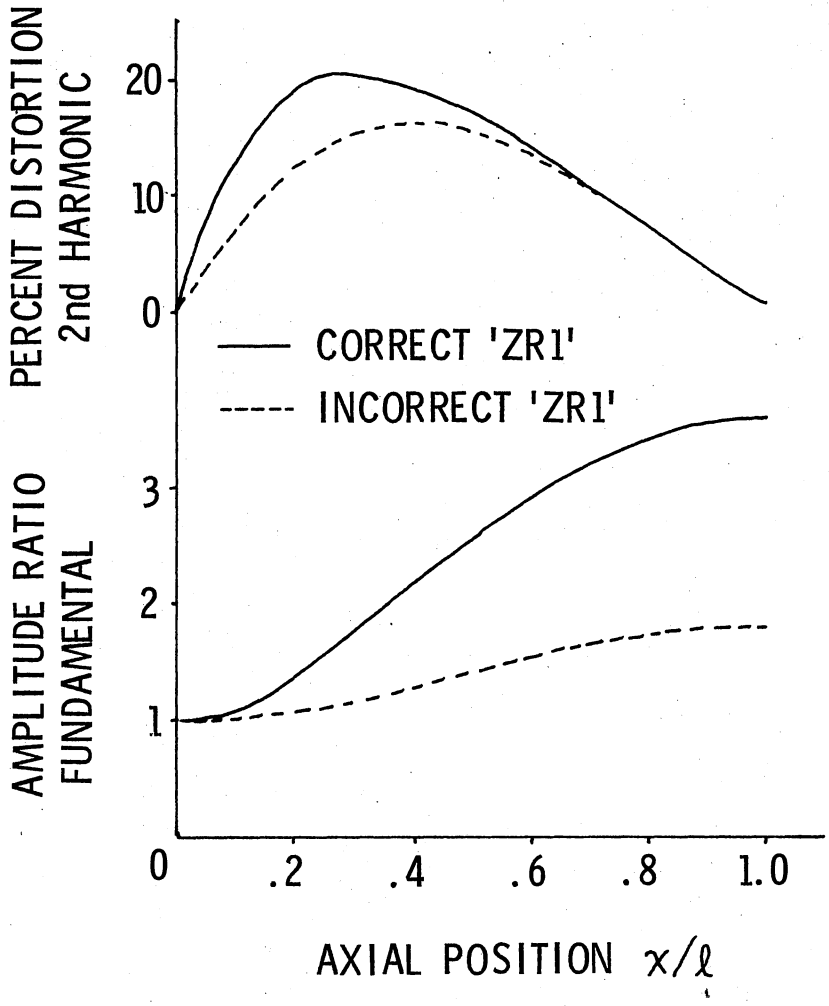

Figure 2. Comparison of Strunk's Solution With the Corrected Solution for FN = 1.6, BCP1 = 0.1, BCP21 = 0.0

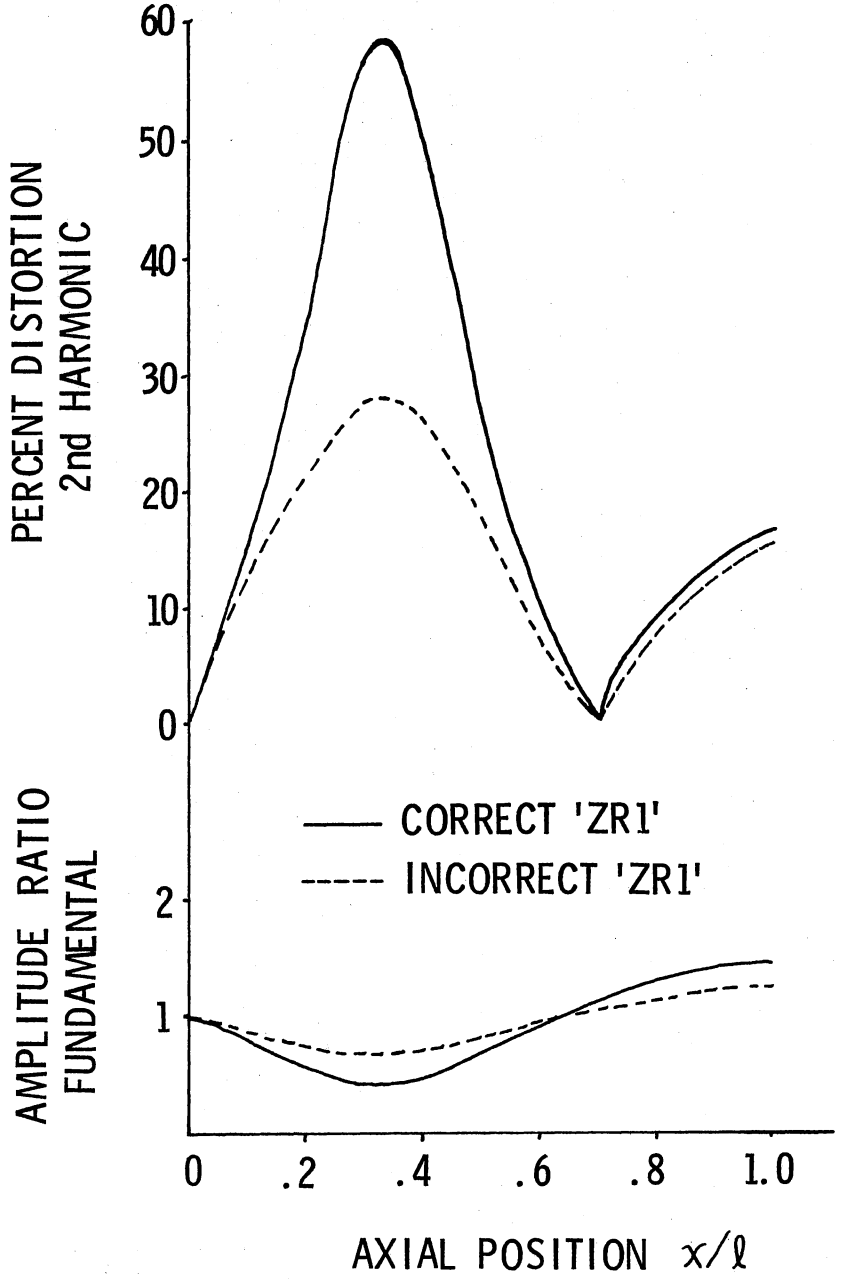

Figure 3. Comparison of Strunk's Solution With the Corrected Solution for FN = 2.3, BCP1 = 0.1, BCP21 = 0.0

From Equation (5.17) it is clear that the percentage second harmonic distortion is directly proportional to the ratio (AQ) of the input flow amplitude to the mean flow amplitude. The results presented in this chapter apply only for one ratio, AQ = 0.5.

A fixed value of 0.6 was considered for the coefficient of discharge C_d.

Figure 4 presents the frequency response of a nonviscous line at $x = \ell$ for different values of the boundary condition parameter BCP1. Linearization of the boundary condition yields an identical plot for the frequency response. The inertance effect of the orifice has been neglected for this plot. From this figure one may notice that for increasing values of the parameter BCP1 the amplification of the fundamental flow response is decreased progressively until a transition point is reached at BCP1 = 0.36. At this point the characteristic impedance of the nonviscous line and the load impedance of the orifice (excluding its inertance effect) are equal. The system is free from the presence of reflected waves if the impedances are matched; hence at BCP1 = 0.36 the amplitude of the fundamental is neither amplified nor attenuated. When the inertance effect of the orifice is neglected, Equation (5.8) reduces to Equation (27) reported by Strunk (3). In this equation the term c(x) is a positive quantity and the term B_1^2 remains numerically greater than unity until the parameter BCP1 crosses the transition value of 0.36. Beyond this transition point B_1^2 is less than unity and hence attenuation of the fundamental flow response results. The corresponding second harmonic distortion for the case of matched impedances is presented in Figure 19.

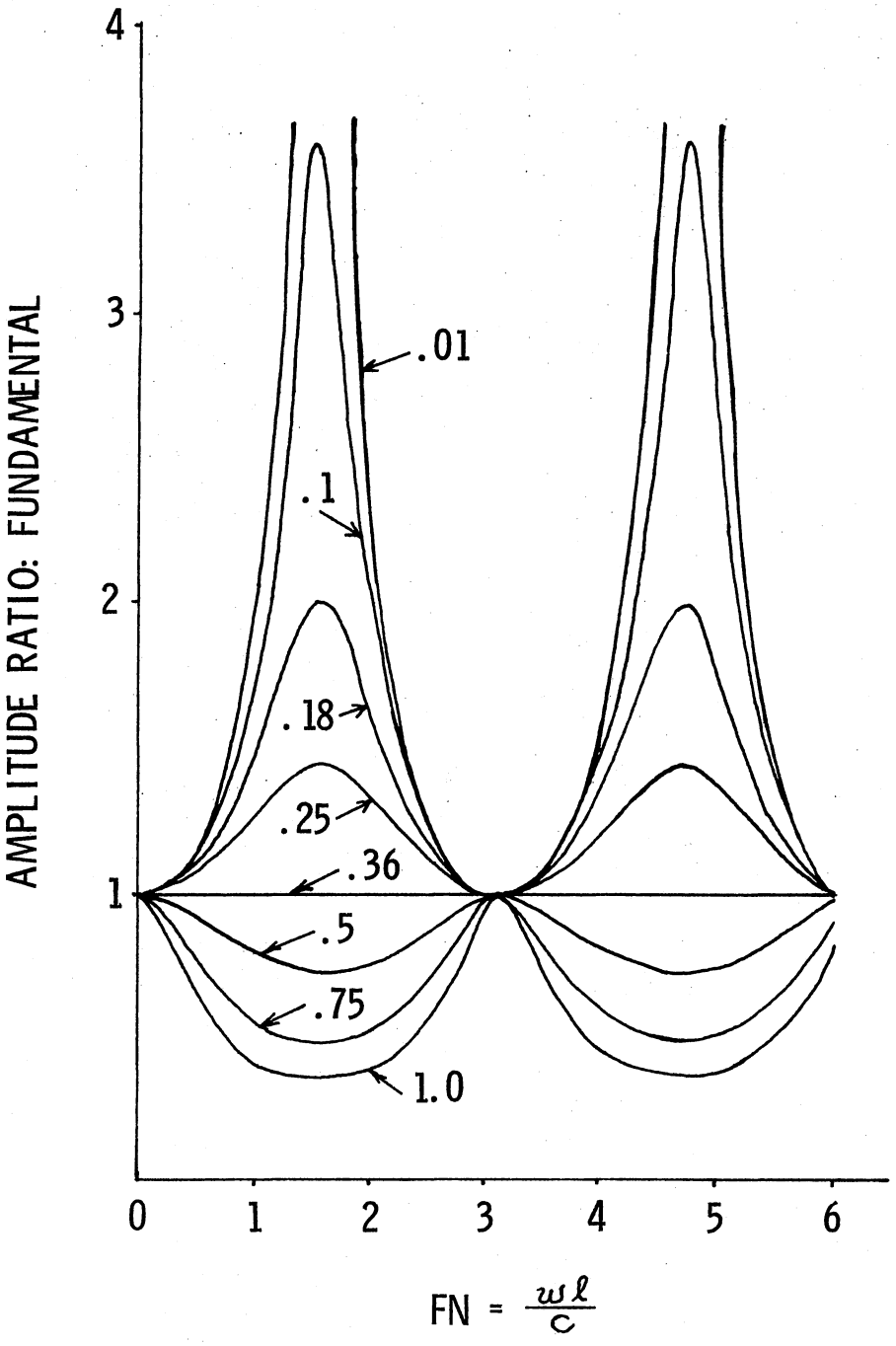

Figure 4. Frequency Response of a Nonviscous Line at x = ℓ for Different Values of BCP1 (BCP21 = 0.0)

The plot designated as 1 in Figure 5 has been reproduced from Figure 4. In Figure 5 the inertance effect of the orifice has been taken into account. The parameter BCP21 exclusively accounts for the inertance effect of the orifice. From Figure 5 one notices that as BCP21 is increased in value numerically, the natural frequencies of the line shift toward the left. The fundamental natural frequency of the line is thus decreased. This is as it should be, because the natural frequency of a linear (distributed) oscillatory system tends to decrease as the inertance effect present at its boundary becomes large. A slight increase in the value of the peak amplitude is also noticeable from Figure 5. Notice that the shift in the natural frequency of the line would be appreciable as the parameter BCP21 assumes values greater than 0.25. Thus the inertance effect of the orifice is appreciable for BCP21 greater than 0.25. For the typical example of line-orifice system considered in Table I the case BCP21 = 0.25 corresponds approximately to a frequency of operation of 700 c/s for a sharp-edged orifice and about 500 c/s for a short-tube orifice.

Figure 6 depicts the percentage second harmonic distortion as a function of frequency number FN for different values of the parameter BCP1. As already noted by Strunk (3) for increasing values of BCP1, the harmonic distortion becomes significant over a broader frequency range.

Plot 1 in Figure 7 has been reproduced from Figure 6 along with other plots which depict the superposition of the inertance effect of the orifice on the percentage second harmonic distortion. The shift in the second harmonic natural frequency is noticeable for increasing values of the parameter BCP21. The peaks, however, are of constant amplitude indicating thereby that peak amplitudes of the second harmonic

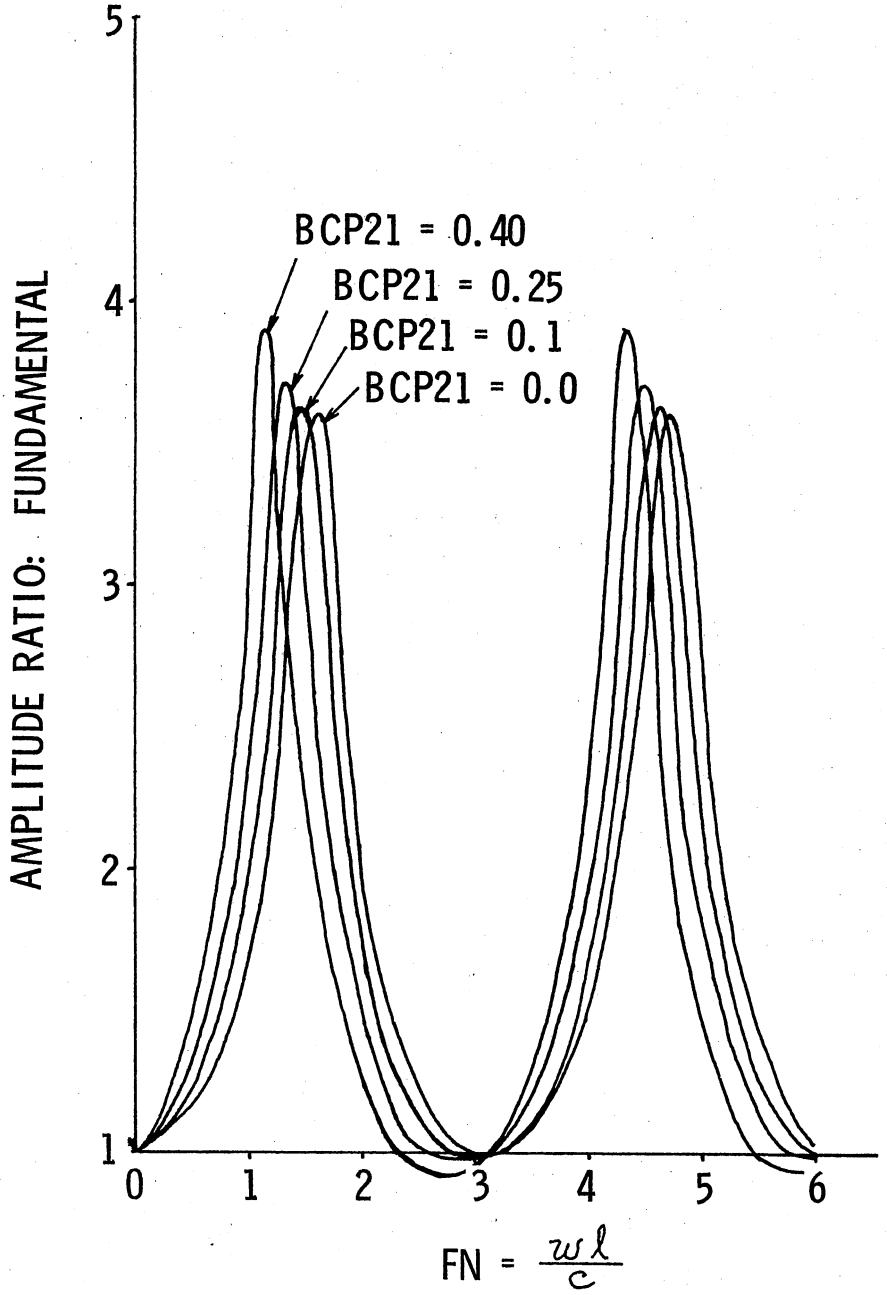

Figure 5. Frequency Response of a Nonviscous Line at x = ℓ for BCP1 = 0.1

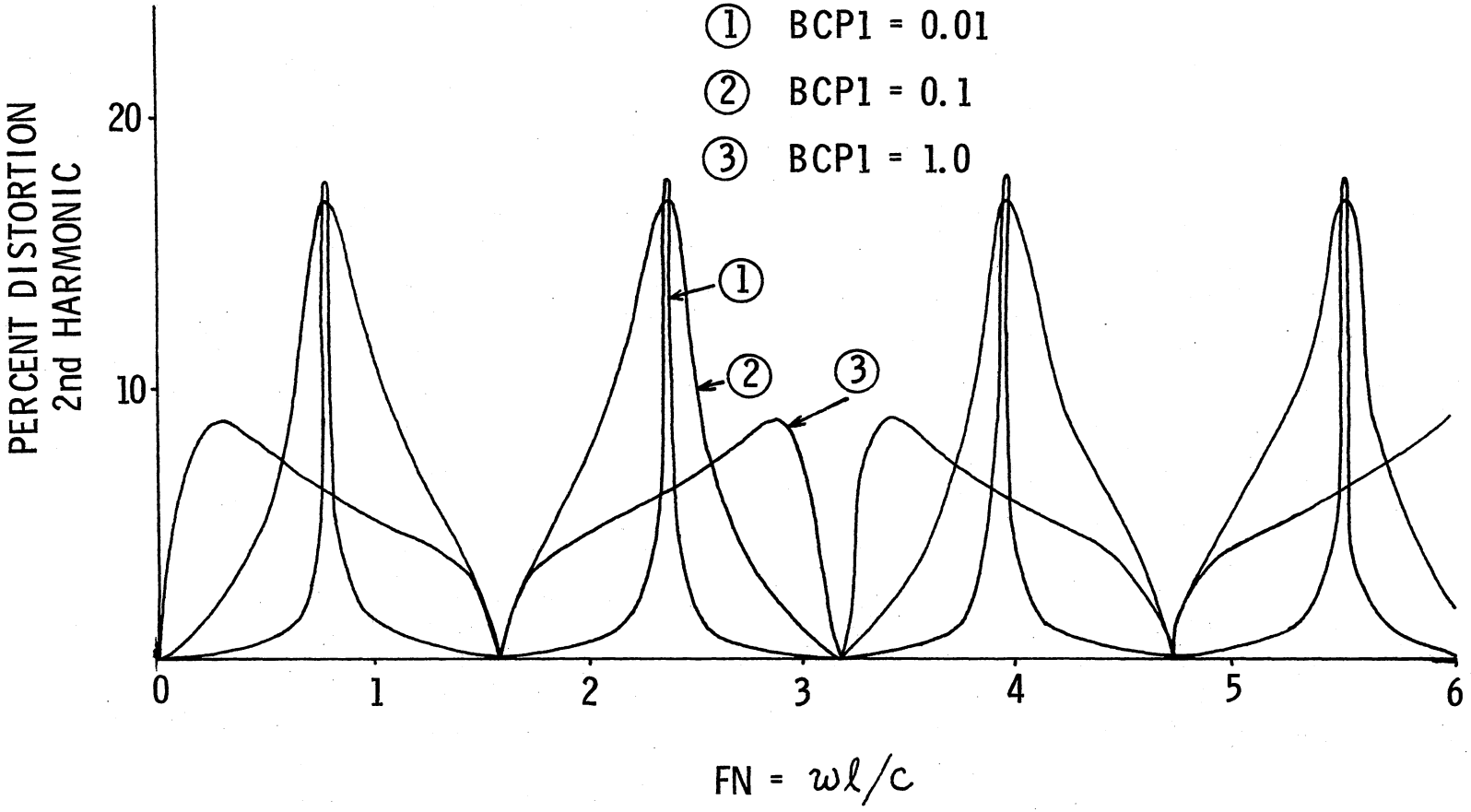

Figure 6. Frequency Response of a Nonviscous Line at x = ℓ for Different Values of BCP1, BCP21 = 0.0

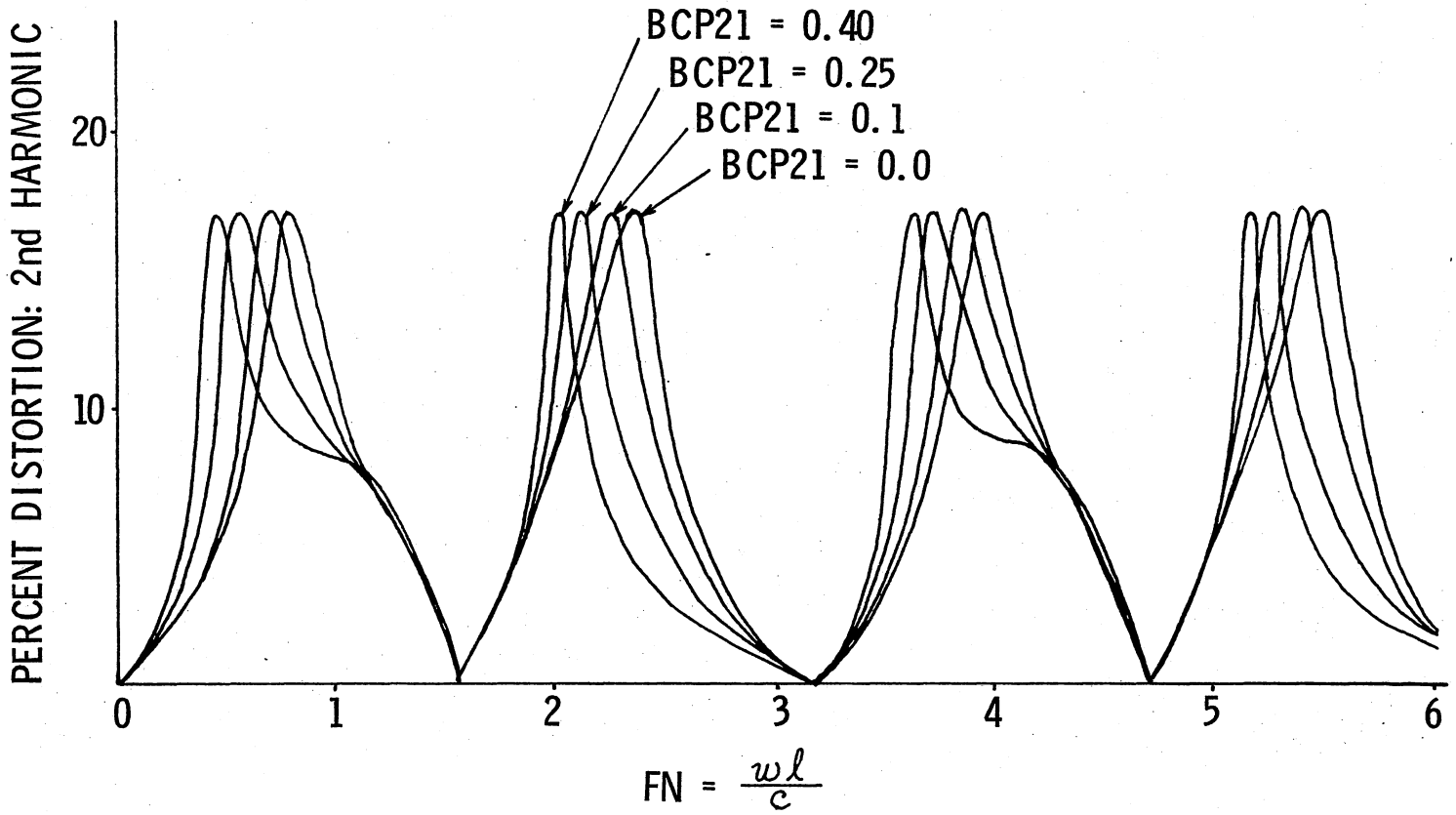

Figure 7. Frequency Response of a Nonviscous Line at x = ℓ for BCP1 = 0.1

are also increasing as the value BCP21 is increased.

Figure 8 depicts the phase response of the fundamental harmonic. It may be noticed that for very low values of the parameter BCP21 the switching point (point where the phase angle switches from a negative value to a positive value) of the phase response coincides with the peak amplitude of the fundamental (Figure 5). However, as the value of BCP21 is increased, this match between the peak amplitude of the fundamental and the switching point of its phase response is lost. Also, it may be noticed that for a given value of the frequency number FN, the effect of increasing the value of the parameter BCP21 leads to an increase in the magnitude of the phase angle. Figure 9 depicts the same phase response but with one difference of the negative phase angles being converted to positive phase angle by the addition of 360° of phase.

Figure 10 depicts the phase response of the second harmonic for BCP1 = 0.1 with two different values for the parameter BCP21. Some of the peaks that appear in this figure have been missed by Strunk (3) due possibly to the use of a larger step-size in the numerical computations. Figure 11 is the corrected version of Figure 5 reported by Strunk (3).

In Figure 12 the amplitude response of the fundamental (for FN = 0.8) as a function of the Axial Position Number XL has been presented along with the superposition of the inertance effect of the orifice. Notice that at $x = \ell$, the amplification of the fundamental flow response increases with increasing values the parameter BCP21. This information is also derivable from Figure 5 if one considers the variation of the amplitude response, at FN = 0.8, for increasing values of the parameter BCP21. Notice again that beyond BCP21 = 0.25 the influence of the

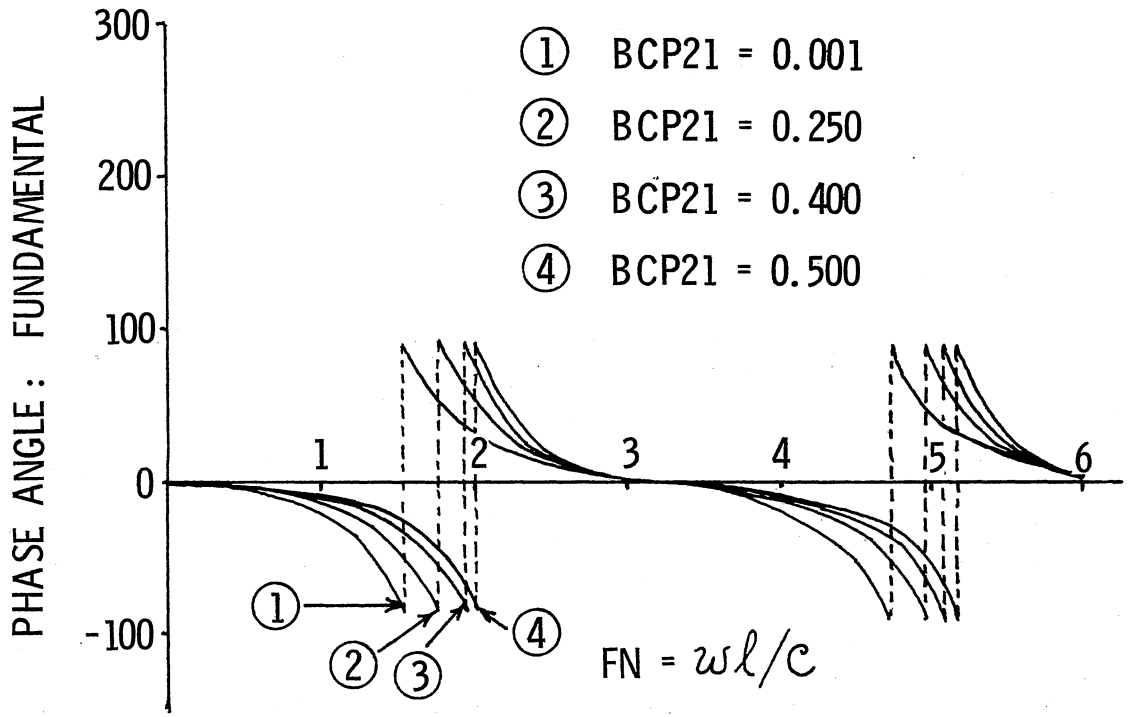

Figure 8. Phase Response of the Fundamental for BCP1 = 0.1

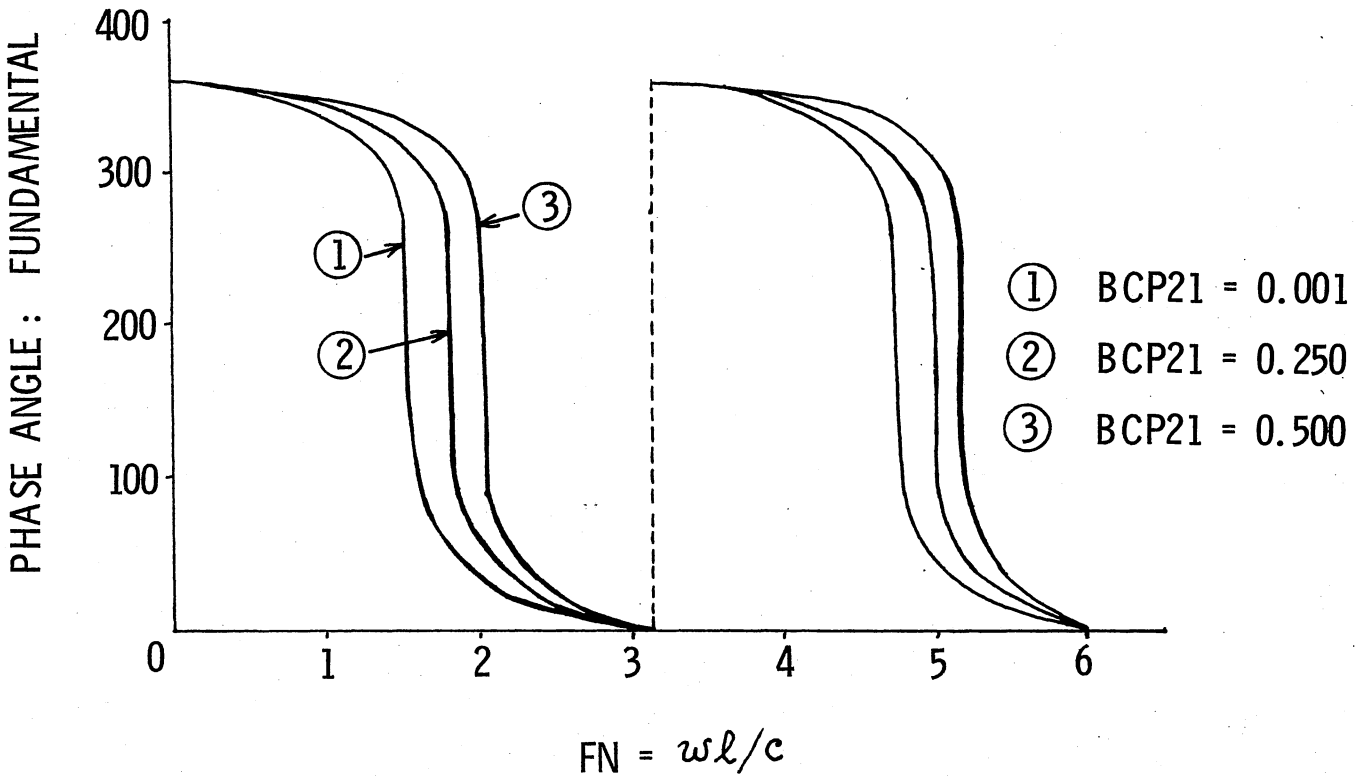

Figure 9. Phase Response of the Fundamental for BCP1 = 0.1 With Phase Angles Expressed as Positive Angles

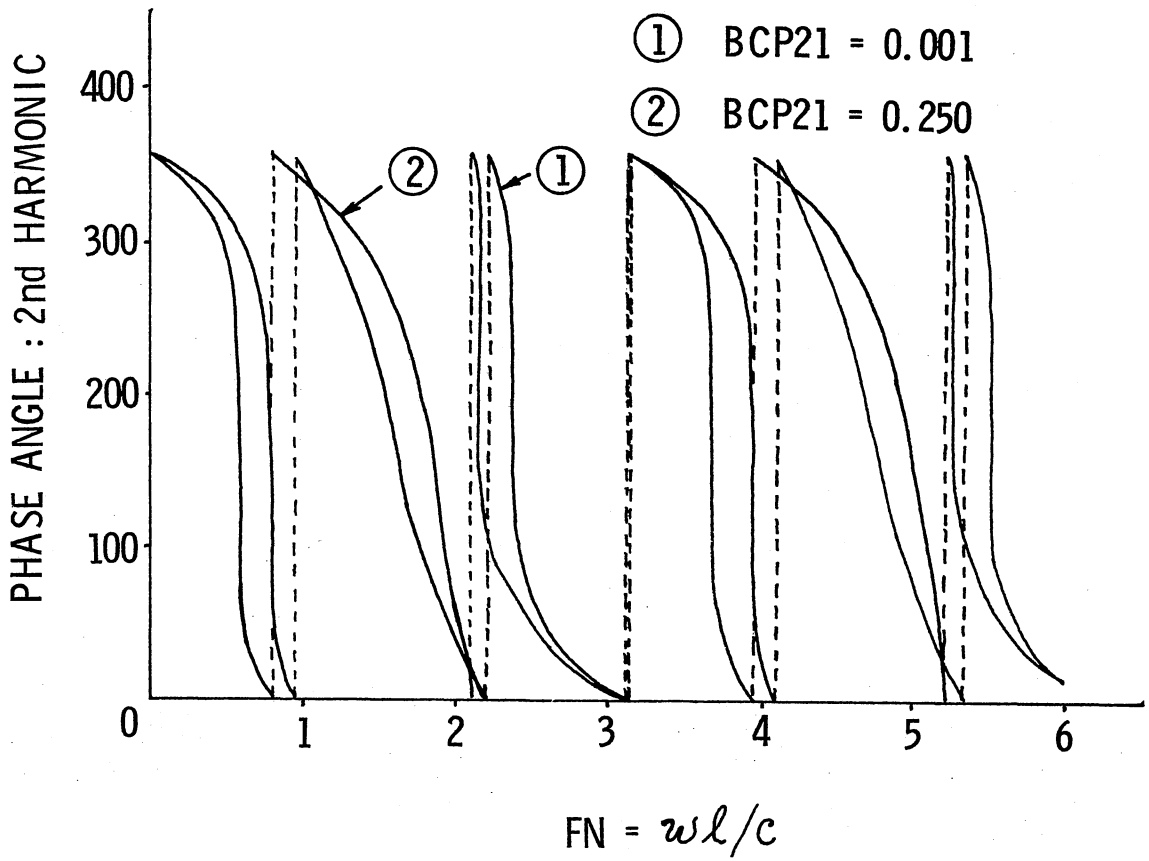

Figure 10. Phase Response of the Second Harmonic for BCP1 = 0.1

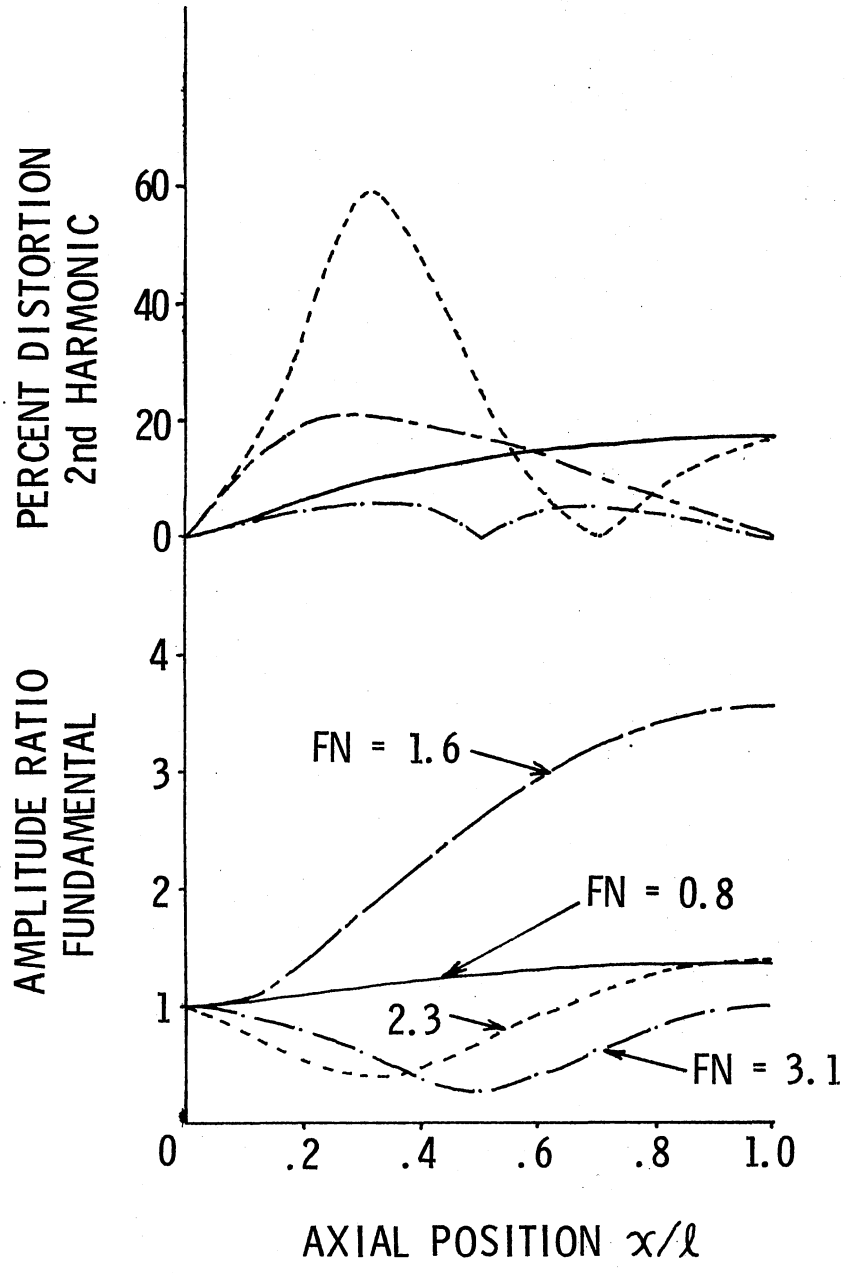

Figure 11. Flow Response of a Nonviscous Line as a Function of Axial Position for BCP1 = 0.1, BCP21 = 0.0

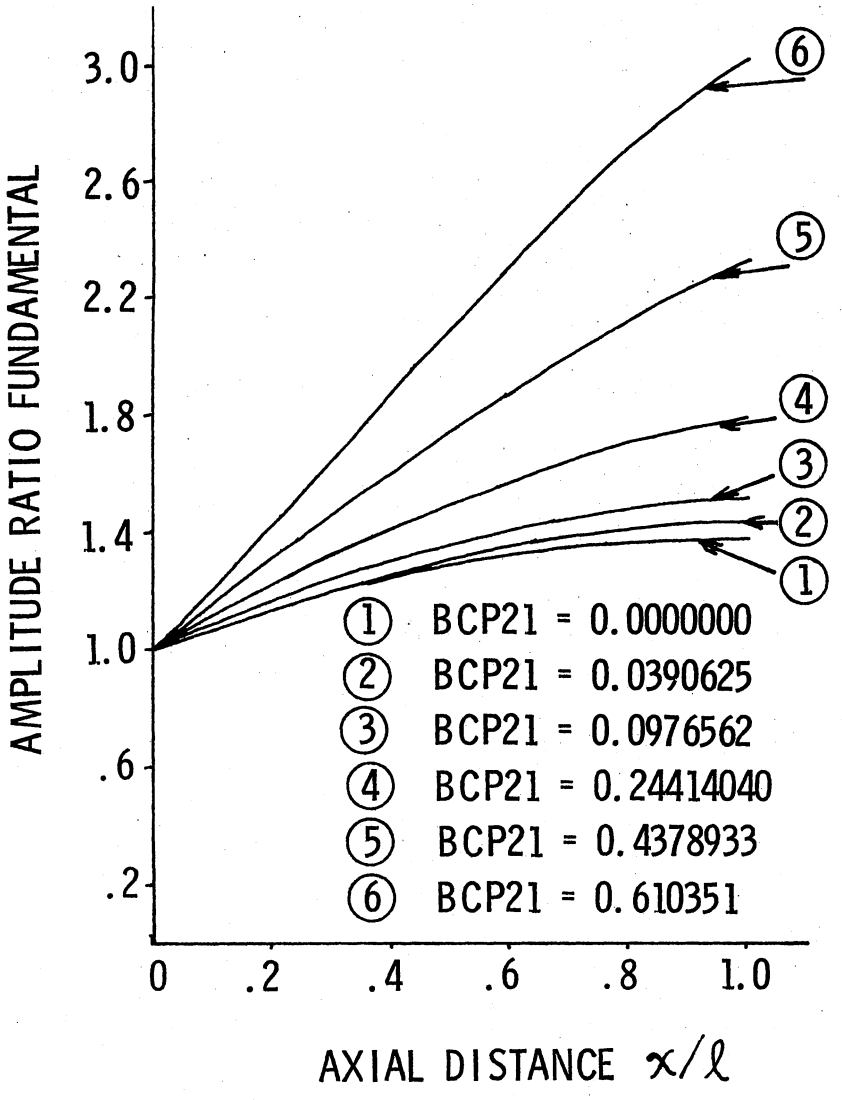

Figure 12. Flow Response of a Nonviscous Line as a Function of Axial Position for BCP1 = 0.1, FN = 0.8

inertance effect of the orifice on the amplitude response is appreciable.

Figure 13 depicts the amplitude response of the fundamental as a function of the axial position for FN = 1.6. The same conclusions as those derived for Figure 12 apply to the discussion of this figure also.

In Figure 14 the percentage second harmonic distortion has been plotted as a function of the axial position number XL for BCP1 = 0.1 and FN = 0.8. Here again one notices that errors of appreciable magnitude are possible in the estimation of the percentage second harmonic distortion for values of BCP21 greater than 0.25. Also for BCP21 = 0.65684 one notices that the amplitude of the second harmonic is of the same order of magnitude as the fundamental. Thus for highly inertive (short-tube) orifices it may be necessary to improve the accuracy of the perturbation solution by considering additional terms of the total solution given by Equation (4.3).

In Figure 15 the percentage second harmonic distortion has been considered as a function of the Axial Position Number XL for BCP1 = 0.1 and FN = 1.6. Notice that for FN = 1.6 no appreciable error in the estimation of the percentage second harmonic distortion results even for very high values of the parameter BCP21. This information is also contained in Figure 6. Thus if the Frequency Number FN assumes a value such that one is operating in the immediate vicinity of the valleys depicted in Figure 6, then the harmonic distortion due to the second harmonic is small and so also is the error introduced by the neglect of the inertance effect of the orifice.

Figures 16, 17 and 18 depict the amplitude response of the fundamental and the percentage second harmonic distortion as a function of the Axial Position Number XL for BCP1 = 1.0. For BCP1 = 1.0 the

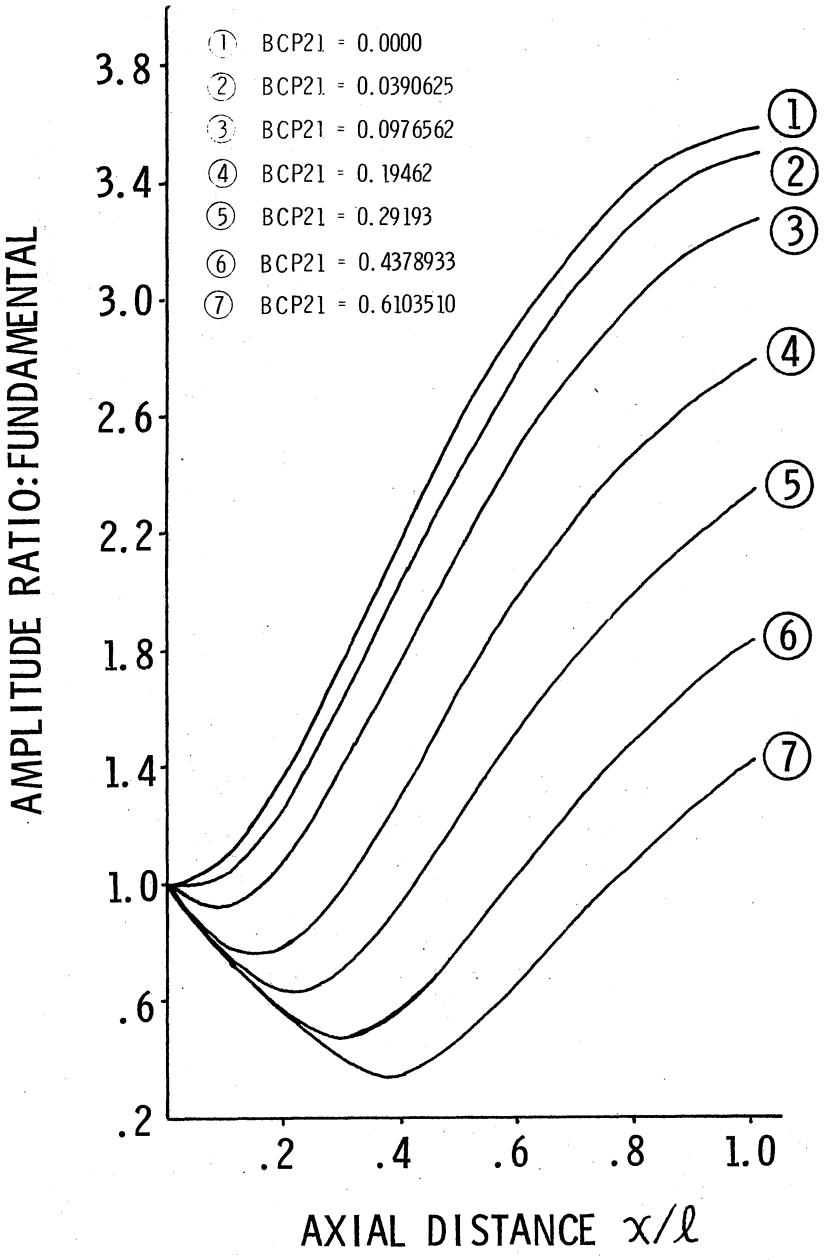

Figure 13. Flow Response of a Nonviscous Line as a Function of Axial Position for BCP1 = 0.1, FN = 1.6

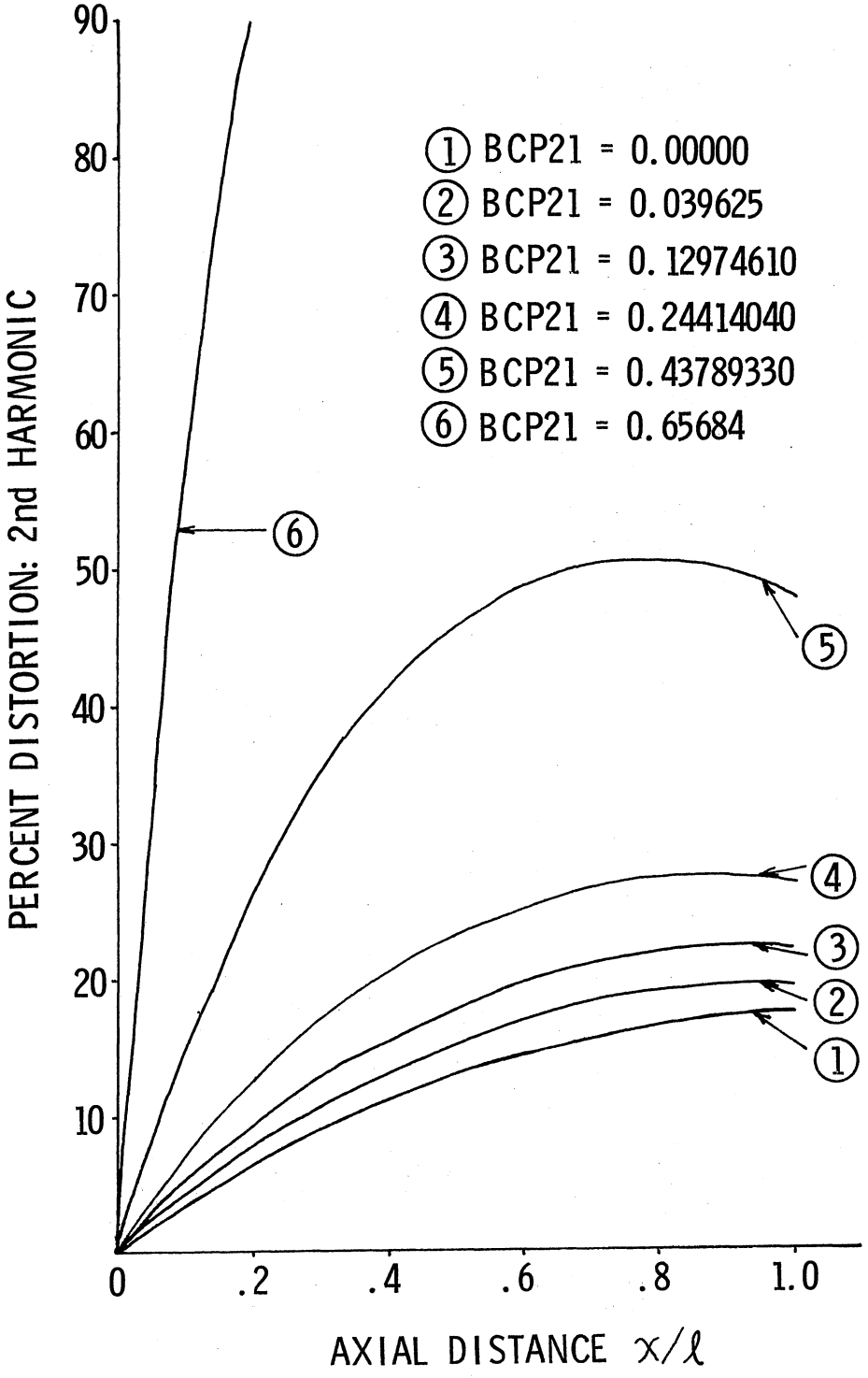

Figure 14. Flow Response of a Nonviscous Line as a Function of Axial Position for BCP1 = 0.1, FN = 0.8

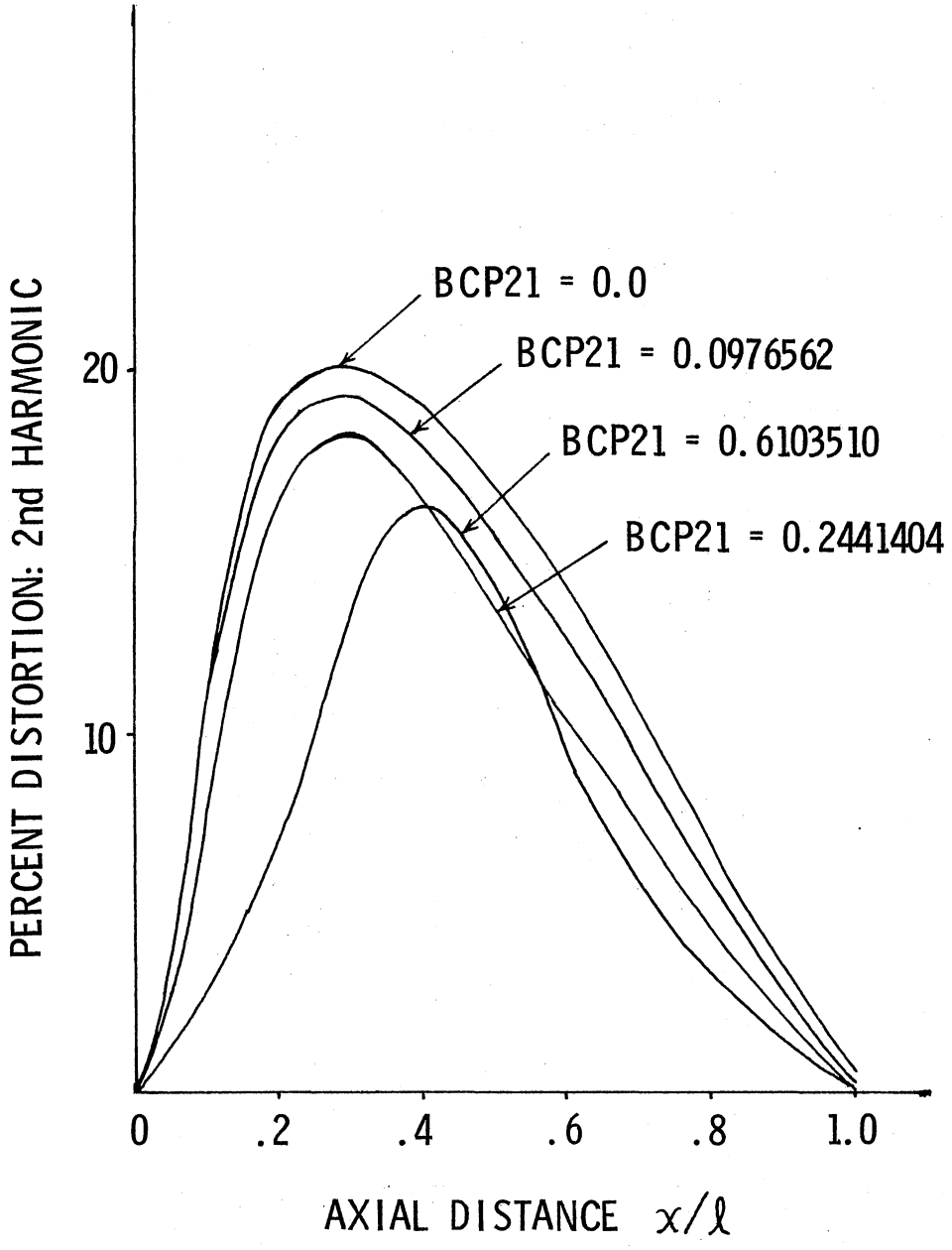

Figure 15. Flow Response of a Nonviscous Line as a Function of Axial Position for BCP1 = 0.1, FN = 1.6

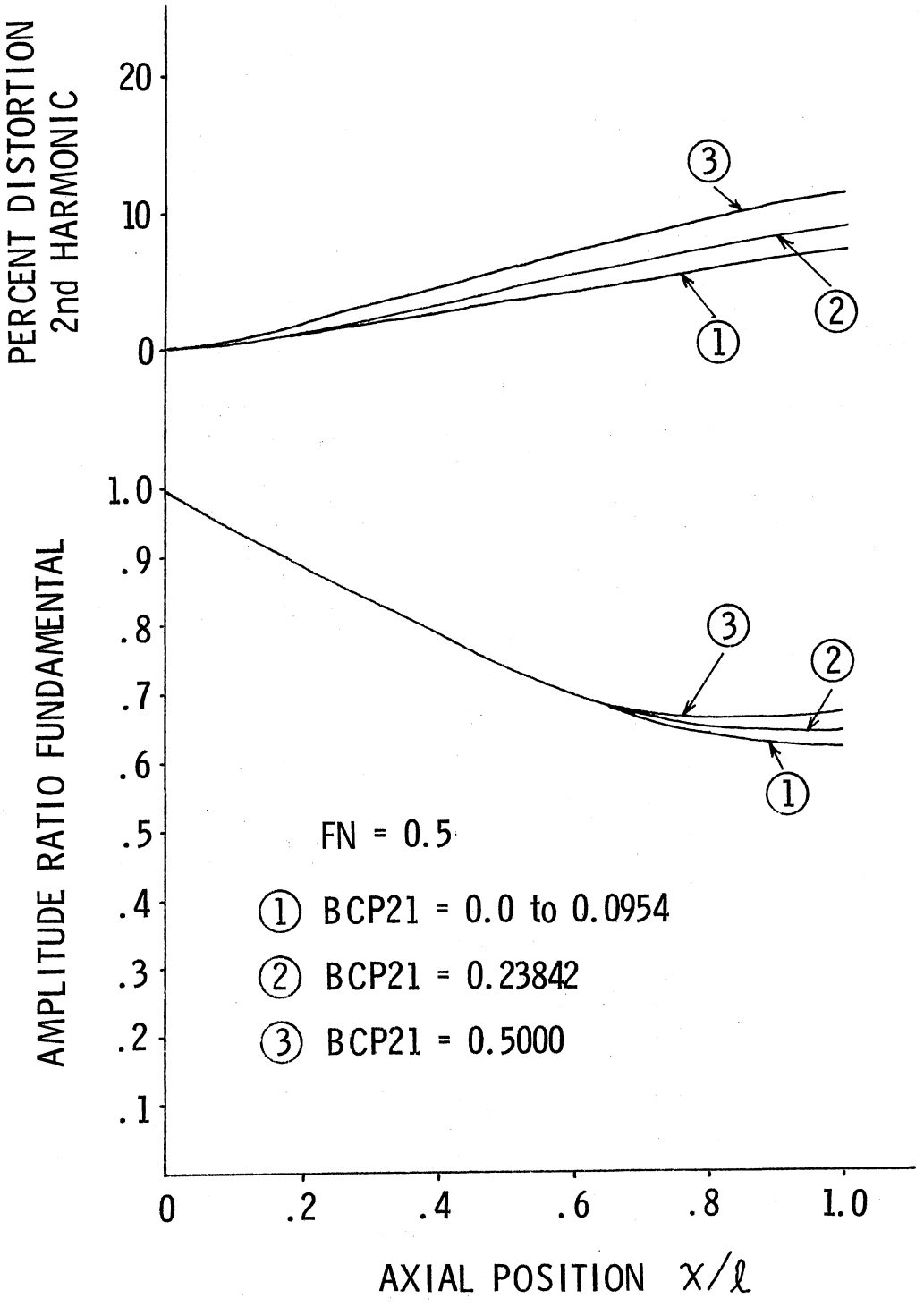

Figure 16. Flow Response of a Nonviscous Line as a Function of Axial Position for BCP1 = 1.0, FN = 0.5

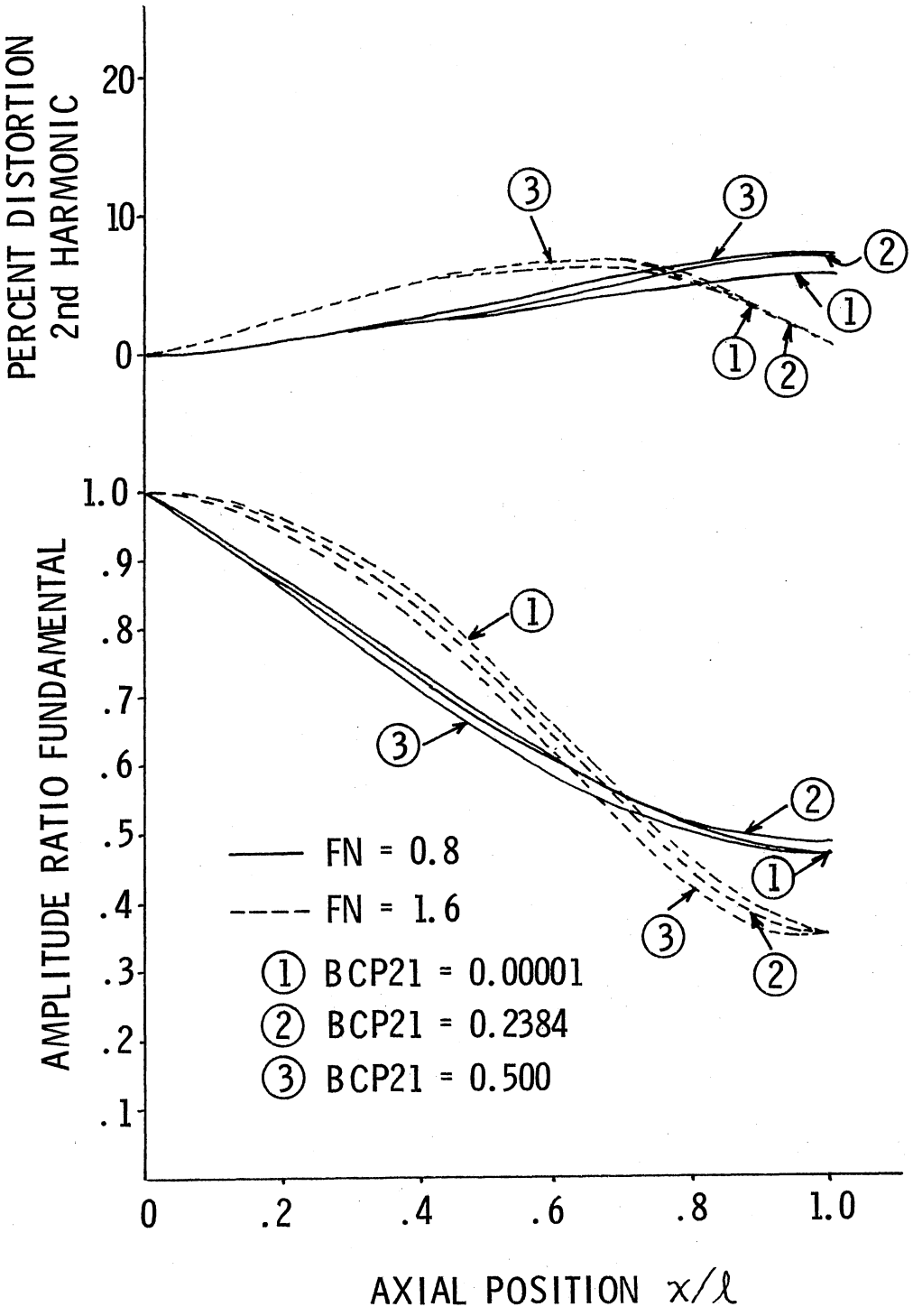

Figure 17. Flow Response of a Nonviscous Line as a Function of Axial Position for BCP1 = 1.0, FN = 0.8 and 1.6

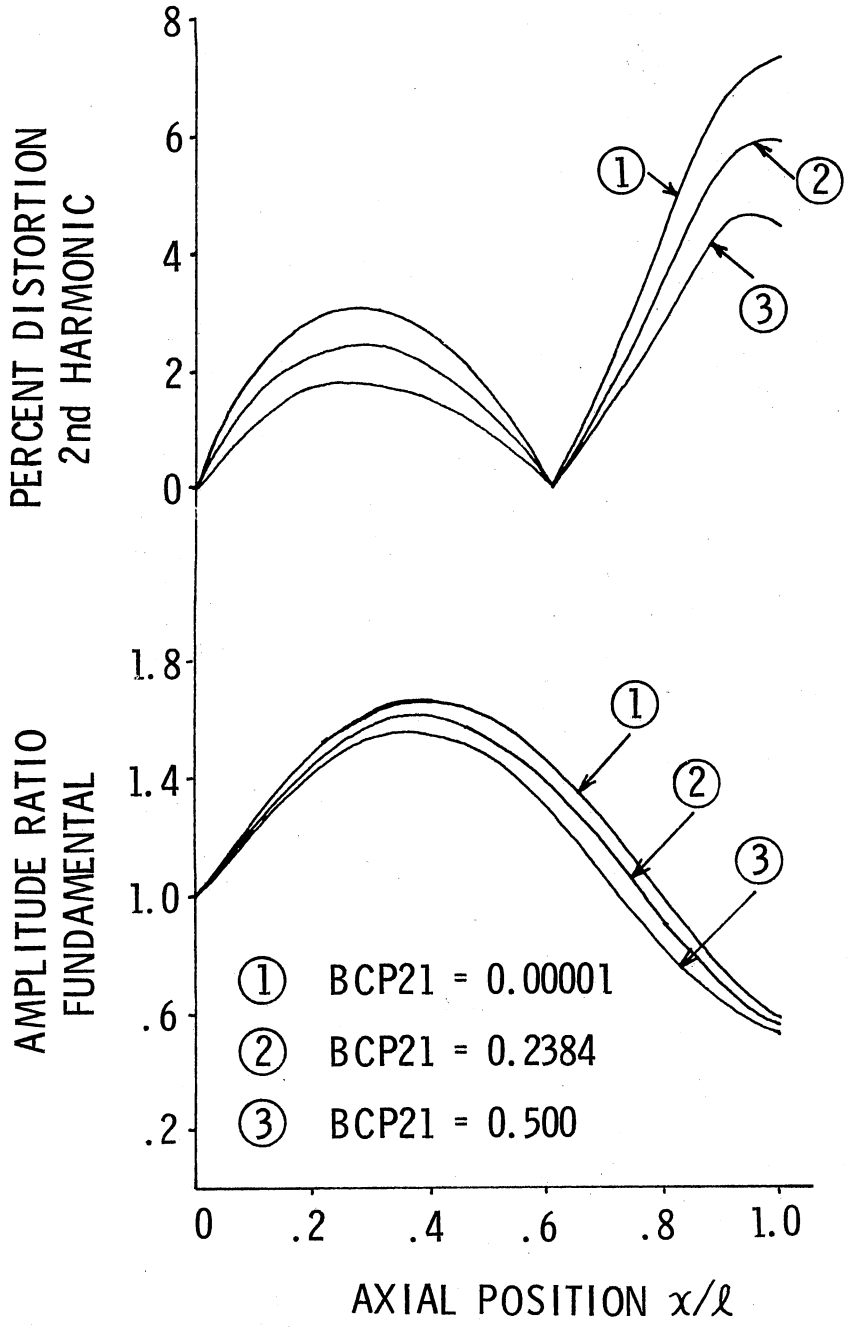

Figure 18. Flow Response of a Nonviscous Line as a Function of Axial Position for BCP1 = 1.0, FN = 2.6

dimensionless ratio ZR1 is greater than unity, hence attenuation of the fundamental flow response results at $x = \ell$. Also it will be noticed that increasing the value of the parameter BCP21 has little influence on the flow response for BCP1 = 1.0. This may be explained by referring to Equation (4.9) which indicates that for BCP21 less than unity and ZR1 greater than unity, the term r_2 is a strong function of ZR1 and therefore increasing values of BCP21 exert only a weak influence on the flow response at BCP1 = 1.0.

This result concerning the influence of the inertance effect of the orifice on the system's frequency response for BCP1 = 1.0 is, strictly speaking, not a valid result, because for small diameter lines, the basic assumption of the Reynold's number being less than or equal to 2000 is violated when the dimensionless ratio BCP1 assumes a value of unity.

Figures 19 and 20 are similar to Figures 4 and 11. The value of the parameter BCP1, however, is now changed to 0.36. As already pointed out, for this value of BCP1, the load impedance of the orifice (with its inertance effect excluded) matches the Characteristic Impedance of the nonviscous line. The amplitude response of the fundamental thus remains constant with frequency. Figures 19 and 20 then indicate the variation of the percentage second harmonic distortion as functions of the Frequency Number FN and the Axial Position Number XL.

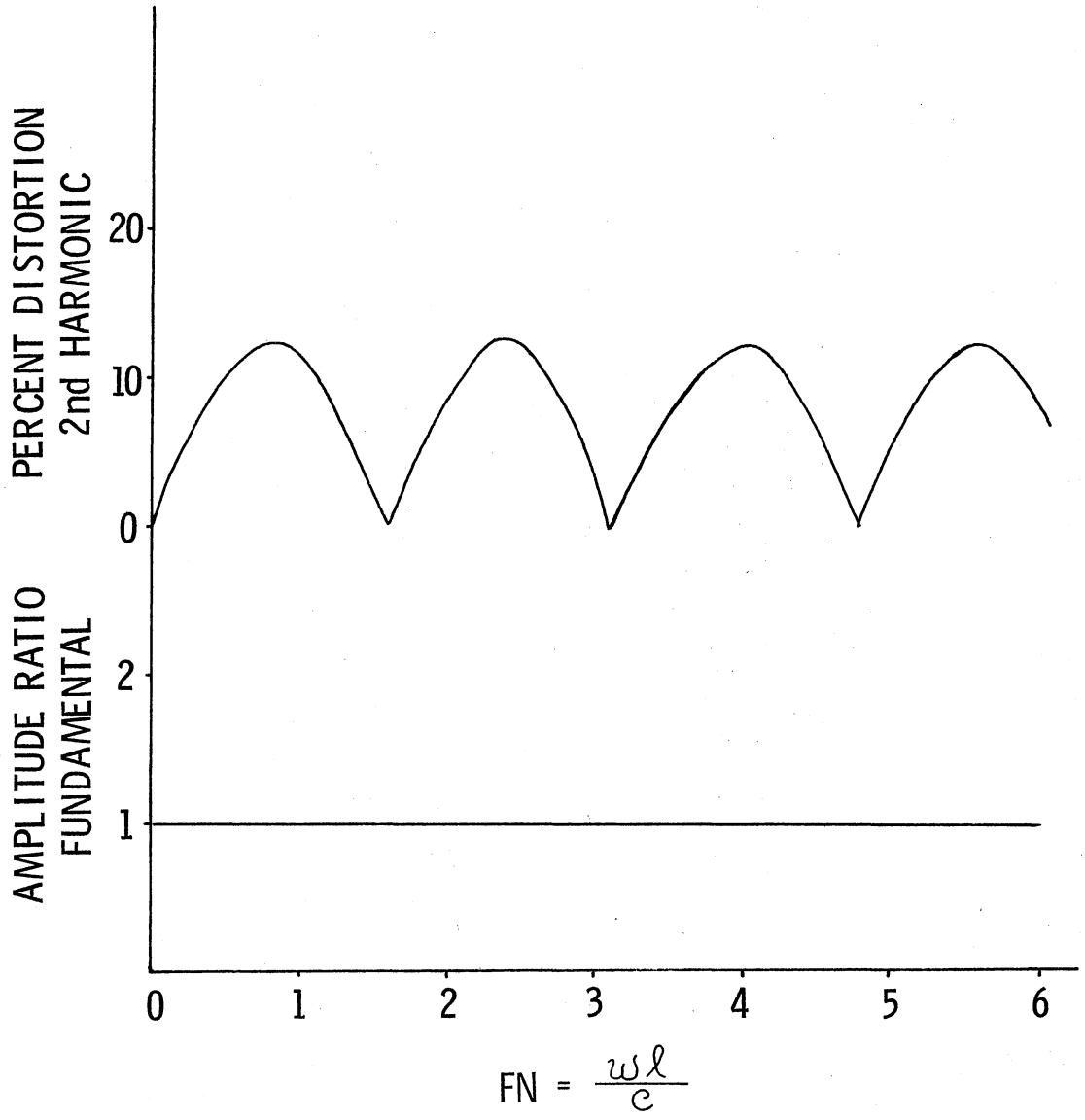

Figure 19. Frequency Response of a Nonviscous Line at x = ℓ as a Function of Frequency Number FN for Matched Impedances, BCP1 = 0.36, BCP21 = 0.0

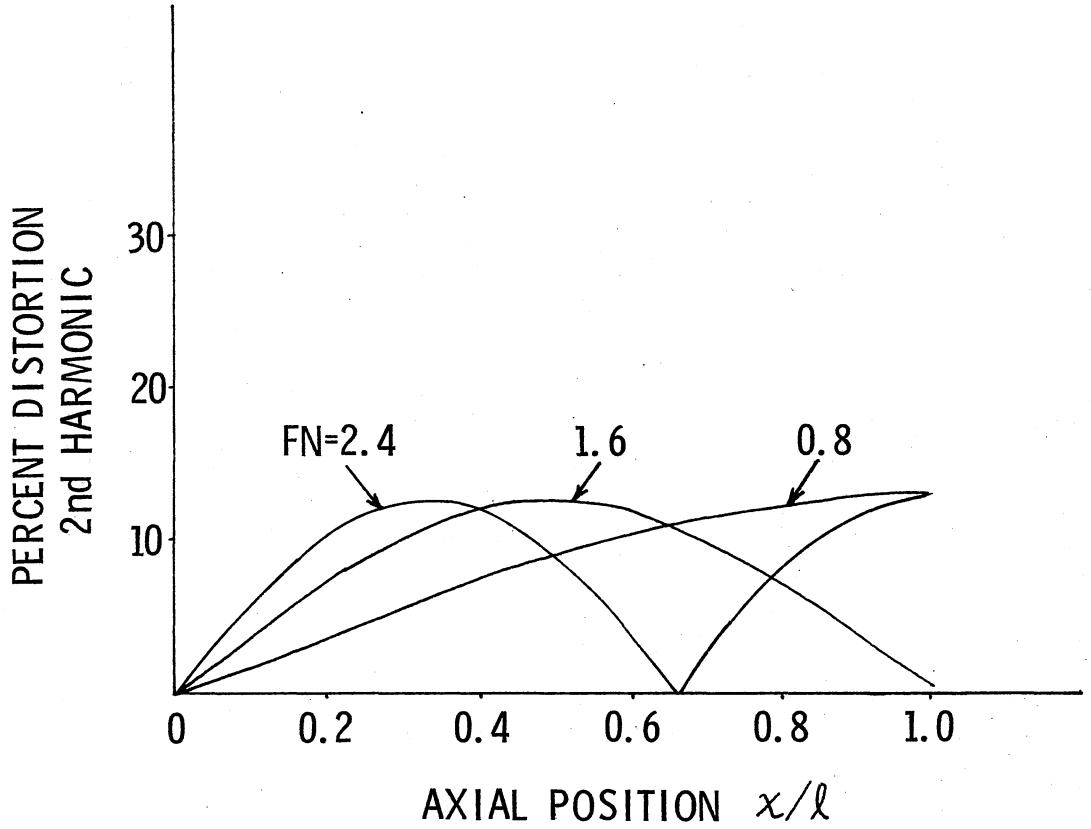

Figure 20. Percent Second Harmonic Distortion as a Function of Axial Position for Matched Impedances, BCP1 = 0.36, BCP21 = 0.0

CHAPTER VII

SUMMARY, CONCLUSIONS AND RECOMMENDATIONS

Summary

This work is an extension of the work earlier reported by Strunk (3) concerning the frequency response of a nonviscous line with a nonlinear boundary condition. In his work, however, the inertance effect of the orifice, which becomes important at high frequencies, has been neglected. The model reported by him therefore remains valid for low frequency perturbations only.

In this thesis a generalized model, which accounts for inertance effect of the orifice, has been developed. This model is applicable for the propagation of both low and high frequency disturbances through the line. At low frequencies, when the inertance effect of the orifice is small, it has been shown that this model reduces, as a special case, to the model reported by Strunk (3).

The orifice-flow model due to Funk et al. (4) has been employed in this work to derive a modified boundary condition for the case of a fluid line terminated by a nonlinear inertive orifice. The nonviscous wave equation has been subsequently solved, subject to this new boundary condition, by applying the Perturbation Method. Closed form nondimensional solutions for the amplitude and phase response of the first and second harmonics have been reported. An important dimensionless number

which exclusively accounts for the inertance effect of the orifice has been identified. Nondimensional plots of the frequency response obtained, as a result of perturbing this dimensionless number, have been presented.

Conclusions

The conclusions which have been reached as a result of this study are:

1. The influence of the inertance effect of the orifice on the frequency response of a nonviscous line may be accounted for by a dimensionless number. This number has been referred to as a boundary condition parameter (BCP21) in this work. It has been found to be a function of the inertance of the orifice (i.e., its physical size, coefficient of discharge, etc.), the physical properties of the fluid, the sonic velocity, the cross-sectional area of the line, and finally the frequency of oscillation of the disturbance.

2. The influence of the inertance effect of the orifice is dependent on yet another dimensionless number, referred to as boundary condition parameter BCP1 in this work. This parameter is a function of the noninertive load impedance of the orifice (i.e., its resistance), and the characteristic impedance of the nonviscous line.

3. For BCP1 = 0.1 it has been found that the inertance effect of the orifice on the frequency response becomes appreciable as BCP21 assumes values in excess of 0.25. For small diameter lines (lines with internal diameter one inch or less) terminated by a sharp-edged orifice, of size in the range 1/8 inch to 1/4 inch, this would generally mean that the inertance effect is appreciable beyond a frequency of operation

of 700 c/s. For short-tube orifices (orifices with thickness in the range 1/8 inch to 1/4 inch) the inertance effect is appreciable beyond a frequency of operation of 500 c/s.

4. The natural frequencies of the line have been found to decrease as the inertance effect of the orifice was made large.

5. Depending on the value of the frequency number FN, the effect of the orifice's inertance is either to amplify or to attenuate the amplitude of the fundamental and the magnitude of the second harmonic distortion.

6. For BCP1 = 0.1, the percentage second harmonic distortion becomes appreciable if (a) the frequency number FN corresponds to a natural frequency of the line, and (b) BCP21 is of a value greater than 0.25. This suggests that at high frequencies of operation it may be necessary to improve the perturbation solution by addition of the third and possibly even the fourth harmonic term.

Recommendations for Future Study

Areas which it is felt are worthy of future study include:

1. Investigation of the frequency response of a viscous fluid line with nonlinear inertive orifice as a boundary condition.

2. Experimental validation of the theory.

A SELECTED BIBLIOGRAPHY

(1) Reid, K. N. "Dynamic Models of Fluid Transmission Lines." Proceedings of the Symposium on Fluidics and Internal Flows. Pennsylvania State University, October 24, 25, 1968.

(2) Goodson, R. E. and R. G. Leonard. "Survey of Modeling Techniques for Fluid Line Transients." Trans. ASME, Journal of Basic Engineering, Vol. 93, No. 3 (June, 1972), pp. 475-482.

(3) Strunk, R. D. "Frequency Response of Fluid Lines with Nonlinear Boundary Condition." Trans. ASME, Journal of Basic Engineering, Vol. 94, No. 2 (September, 1971), pp. 365-372.

(4) Funk, J. E. et al. "The Transient Response of Orifices and Very Short Lines." Trans. ASME, Journal of Basic Engineering, Vol. 94, No. 2 (June, 1972), pp. 483-491.

(5) Lahey, R. T., Jr. and B. S. Shiralkar. "Transient Flow Measurements with Sharp-Edged Orifices." Fluid Dynamic Measurements, ASME publication (1971), pp. 1-5.

(6) Yellin, E. L. and C. S. Peskin. "Large Amplitude Pulsatile Flow Across an Orifice." Trans. ASME, Journal of Dynamic Systems Measurement and Control, Vol. 97, No. 1 (March, 1975), pp. 92-95.

(7) D'Souza, A. F. and R. Oldenburger. "Dynamic Response of Fluid Lines." Trans. ASME, Journal of Basic Engineering, Vol. 86 (September, 1964), pp. 589-598.

(8) Gerlach, C. R. "The Dynamics of Viscous Fluid Transmission Lines with Particular Emphasis on Higher Mode Propagation." (Ph.D. dissertation, School of Mechanical and Aerospace Engineering, Oklahoma State University, Stillwater, Oklahoma, July, 1966.)

(9) Brown, F. T. "The Transient Response of Fluid Lines." Trans. ASME, Journal of Basic Engineering, Vol. 84 (December, 1962), pp. 547-553.

(10) Kinsler, L. E. and A. R. Frey. Fundamentals of Acoustics. New York: John Wiley & Sons, Inc., 1962.

(11) Rouleau, W. T. "Pressure Surges in Pipelines Carrying Viscous Liquids." Trans. ASME, Journal of Basic Engineering, Vol. 82 (October, 1960), pp. 912-920.

(12) Streeter, V. L. and E. B. Wylie. Hydraulic Transients. New York: McGraw-Hill Book Co., Inc., 1967.

APPENDIX A

SETS OF LINEAR SYSTEM EQUATIONS

Substituting Equation (4.3) in Equations (4.1) and (4.2) one obtains

$$[q_{tt}^{(o)} + \varepsilon\, q_{tt}^{(1)} + \varepsilon^2\, q_{tt}^{(2)} + \varepsilon^3\, q_{tt}^{(3)} + \ldots + \ldots] - c^2\,[q_{xx}^{(o)} + \varepsilon\, q_{xx}^{(1)} + \varepsilon^2\, q_{xx}^{(2)} + \varepsilon^3\, q_{xx}^{(3)} + \ldots + \ldots] = 0. \tag{A.1}$$

$$[q^{(o)} + \varepsilon\, q^{(1)} + \varepsilon^2\, q^{(2)} + \ldots]_{x\,=\,0} = A\sin(\omega t). \tag{A.2}$$

$$[\{q_x^{(o)} + \varepsilon\, q_x^{(1)} + \varepsilon^2\, q_x^{(2)} + \ldots\} + \alpha\{q_t^{(o)} + \varepsilon\, q_t^{(1)} + \varepsilon^2\, q_t^{(2)} + \ldots\} + \beta\,\{q_{tt}^{(o)} + \varepsilon\, q_{tt}^{(1)} + \varepsilon^2\, q_{tt}^{(2)}\}]_{x\,=\,\ell} = -\varepsilon\,[\{q^{(o)} + \varepsilon\, q^{(1)} + \varepsilon^2\, q^{(2)} + \ldots\}\{q_t^{(o)} + \varepsilon\, q_t^{(1)} + \varepsilon^2\, q_t^{(2)} + \ldots\}]_{x\,=\,\ell}. \tag{A.3}$$

Equating terms with like powers of "ε" in Equations (A.1), (A.2) and (A.3), the following sets of linear partial differential equations with linear boundary conditions are obtained.

For $O(\varepsilon = 0)$,

$$q_{tt}^{(o)} - c^2\, q_{xx}^{(o)} = 0$$

At $x = 0$,

$$q^{(o)}\,(0, t) = A\sin(\omega t) \tag{A.4}$$

At $x = \ell$,

$$q_x^{(o)} + \alpha\, q_t^{(o)} + \beta\, q_{tt}^{(o)} = 0$$

For $O(\varepsilon)$,

$$q_{tt}^{(1)} - c^2 \cdot q_{xx}^{(1)} = 0$$

At $x = 0$,

$$q^{(1)}\,(0,\, t) = 0 \tag{A.5}$$

At $x = \ell$,

$$q_x^{(1)} + \alpha\, q_t^{(1)} + \beta\, q_{tt}^{(1)} = -q^{(o)}\, q_t^{(o)}$$

For $O(\varepsilon^2)$,

$$q_{tt}^{(2)} - c^2\, q_{xx}^{(2)} = 0$$

At $x = 0$,

$$q^{(2)}\,(0,\, t) = 0 \tag{A.6}$$

At $x = \ell$,

$$q_x^{(2)} + \alpha\, q_t^{(2)} + \beta\, q_{tt}^{(2)} = -\{q^{(o)}\, q_t^{(1)} + q^{(1)}\, q_t^{(o)}\}$$

For $O(\varepsilon^3)$,

$$q_{tt}^{(3)} - c^2\, q_{xx}^{(3)} = 0$$

At $x = 0$,

$$q^{(3)}\,(0,\, t) = 0 \tag{A.7}$$

At $x = \ell$,

$$q_x^{(3)} + \alpha\, q_t^{(3)} + \beta\, q_{tt}^{(3)} = -\{q^{(o)}\, q_t^{(2)} + q^{(1)}\, q_t^{(1)} + q^{(2)}\, q_t^{(o)}\}$$

and so on.

APPENDIX B

AN EQUATION DEFINING "λ"

Consider the elementary wave equation,

$$q_{tt} - c^2 q_{xx} = 0 \tag{B.1}$$

Let

$$q = X(x) \cdot T(t) \tag{B.2}$$

where X is a function of "x" alone and T is a function of "t". Substituting Equation (B.2) in Equation (B.1) and separating the variables, one obtains

$$\frac{1}{c^2} \frac{T_{tt}}{T} = \frac{X_{xx}}{X} = -\lambda^2$$

where $-\lambda^2$ is a constant of separation. We thus obtain:

$$T_{tt} + (\lambda^2 c^2) T = 0 \tag{B.3}$$

$$X_{xx} + \lambda^2 X = 0 \tag{B.4}$$

For purposes of frequency analysis (i.e., for steady oscillatory flow case), we assume a harmonic solution for T.

Let,

$$T = C_3 e^{i\omega t} \tag{B.5}$$

Substituting Equation (B.5) in Equation (B.3), we have

$$C_3 (-\omega^2) e^{i\omega t} + \lambda^2 c^2 C_3 e^{i\omega t} = 0$$

Simplifying and considering the positive root of λ, we have

$$\lambda = \omega/c \tag{B.6}$$

Equation (B.4) has a solution

$$X = C_1 e^{i\lambda x} + C_2 e^{-i\lambda x} \tag{B.7}$$

Substituting Equations (B.5) and (B.7) in Equation (B.2),

$$q_{(x,\ t)} = C_4 e^{i(\omega t+\lambda x)} + C_5 e^{i(\omega t-\lambda x)} \tag{B.8}$$

where C_4 and C_5 are complex constants.

APPENDIX C

SOLUTION FOR $q^{(o)}(x, t)$

Consider the set

$$q_{tt}^{(o)} - c^2 q_{xx}^{(o)} = 0 \tag{C.1}$$

At $x = 0$,

$$q^{(o)} = A \sin(\omega t)$$

$$= \text{Im}\,[A\, e^{i\omega t}] \tag{C.2}$$

At $x = \ell$,

$$q_x^{(o)} + \alpha q_t^{(o)} + \beta q_{tt}^{(o)} = 0 \tag{C.3}$$

Assume a solution of the form,

$$q^{(o)}(x, t) = F\, e^{i(\omega t + \lambda x)} + G\, e^{i(\omega t - \lambda x)} \tag{C.4}$$

where F and G are complex constants and $\lambda = \omega/c$. Using a complex exponential representation for the boundary conditions, we have

At $x = 0$,

$$\text{Im}(F+G)\, e^{i\omega t} = \text{Im}[A\, e^{i\omega t}] \tag{C.5}$$

where Im refers to the Imaginary part of, and A is a real number. In the above equation, since the imaginary part of Equation (C.4) satisfies the boundary condition at $x = 0$, it is to be expected that the imaginary part of $q^{(o)}(x, t)$ will be the actual solution to the generating system (Equation (4.4)).

From Equation (C.5), we have

$$F + G = A \tag{C.6}$$

Next, consider the boundary condition at $x = \ell$. We have

$$q_x^{(o)}(\ell, t) = i\lambda[F\, e^{i(\omega t + \lambda\ell)} - G\, e^{i(\omega t - \lambda\ell)}] \tag{C.7}$$

$$q_t^{(o)}(\ell, t) = i\omega[F\, e^{i(\omega t + \lambda\ell)} + G\, e^{i(\omega t - \lambda\ell)}] \tag{C.8}$$

$$q_{tt}^{(o)}(\ell, t) = -\omega^2[F\, e^{i(\omega t + \lambda\ell)} + G\, e^{i(\omega t - \lambda\ell)}] \tag{C.9}$$

Substituting Equations (C.7, C.8 and C.9) in Equation (C.3) and rearranging terms yield:

$$\frac{F}{G} = \left[\frac{1 - \alpha c - i(\beta c\omega)}{1 + \alpha c + i(\beta c\omega)}\right]$$

$$= H\, e^{i(2\lambda\ell)} \tag{C.10}$$

where

$$H = \frac{1 - \alpha c - i(\beta c\omega)}{1 + \alpha c + i(\beta c\omega)} \tag{C.11}$$

$$H = \left[\frac{r_1}{(1 + \alpha c)^2 + (\beta c\omega)^2}\right] e^{i\theta} \tag{C.12}$$

where

$$r_1 = [\{1 - (\alpha c)^2 - (\beta c\omega)^2\}^2 + 4(\beta c\omega)^2]^{1/2} \tag{C.13}$$

$$\theta = \tan^{-1}\left[\frac{-2\beta c\omega}{1 - \alpha^2 c^2 - (\beta c\omega)^2}\right] \tag{C.14}$$

Let

$$r_2 = \frac{r_1}{(1 + \alpha c)^2 + (\beta c\omega)^2} \tag{C.15}$$

From Equations (C.15, C.12 and C.10),

$$\frac{F}{G} = r_2\, e^{-i(2\lambda\ell - \theta)} \tag{C.16}$$

Eliminating F from Equations (C.6) and (C.16),

$$G = \frac{A[1 + r_2 e^{i(2\lambda\ell-\theta)}]}{1 + 2r_2 \cos(2\lambda\ell-\theta) + r_2^2} \tag{C.17}$$

Rewriting Equation (C.4) as

$$q^{(o)}(x, t) = G[\frac{F}{G} e^{i(\omega t+\lambda x)} + e^{i(\omega t-\lambda x)}] \tag{C.18}$$

and substituting Equations (C.16) and (C.17) in Equation (C.18), and considering the imaginary part of $q^{(o)}(x, t)$ to be the true solution, one obtains

$$q^{(o)}(x, t) = A[\langle\cos(\lambda x) + \frac{2r_2 \sin(2\lambda\ell-\theta)}{1 + 2r_2 \cos(2\lambda\ell-\theta) + r_2^2} \sin(\lambda x)\rangle$$

$$\sin(\omega t) + \langle\frac{(r_2^2-1) \sin(\lambda x)}{1 + 2r_2 \cos(2\lambda\ell-\theta) + r_2^2}\rangle \cos(\omega t)]. \tag{C.19}$$

APPENDIX D

DERIVATION OF STRUNK'S SOLUTION ($\beta = 0$) FOR $q^{(o)}(x, t)$

From Equation (C.14) we notice that when the inertance effect of the orifice is neglected ($\beta = 0$),

$$\theta = 0$$

and from Equation (C.11), the expression for H reduces to

$$H = \left(\frac{1 - \alpha c}{1 + \alpha c}\right) \tag{D.1}$$

Similarly, from Equation (C.13),

$$r_1 = [1 - (\alpha c)^2] \tag{D.2}$$

and

$$r_2 = [1 - (\alpha c)^2]/[1 + \alpha c]^2$$

$$= \left[\frac{1 - \alpha c}{1 + \alpha c}\right] = H \tag{D.3}$$

Equation (C.19) then reduces to

$$q^{(o)}(x, t) = A\left[\left\langle \cos(\lambda x) + \frac{2H \sin(2\lambda \ell)}{1 + 2H \cos(2\lambda \ell) + H^2} \sin(\lambda x) \right\rangle \sin(\omega t) + \frac{(H^2 - 1) \sin(\lambda x) \cos(\omega t)}{1 + 2H \cos(2\lambda \ell) + H^2}\right] \tag{D.4}$$

Substituting Equation (D.1) in Equation (D.4) and expressing $\sin(2\lambda \ell)$ as $2\sin(\lambda \ell) \cos(\lambda \ell)$, one obtains

$$q^{(o)}(x, t) = A\left[\left\langle \cos(\lambda x) + \frac{(1 - \alpha^2 c^2) \sin(\lambda \ell) \cos(\lambda \ell)}{\cos^2(\lambda \ell) + \alpha^2 c^2 \sin^2(\lambda \ell)} \sin(\lambda x) \right\rangle\right.$$

$$\sin(\omega t) - \left\langle \frac{(\alpha c)\cdot \sin(\lambda x)}{\cos^2(\lambda \ell) + \alpha^2 c^2 \sin^2(\lambda \ell)} \right\rangle \cos(\omega t)] \qquad \text{(D.5)}$$

Equation (D.5) is the same Equation (23) reported by Strunk (3).

APPENDIX E

AN EXPRESSION FOR $q^{(o)}(\ell, t)$

Substituting $x = \ell$ in Equation (4.7) and rearranging terms, the resultant equation may be written in the form

$$q^{(o)}(\ell, t) = (A \cdot B_3)[\sqrt{\eta^2 + \xi^2}\ \{\sin(\lambda\ell + \phi_o)\}\sin(\omega t) + \{(r_2^2 - 1)\sin(\lambda\ell)\}\cos(\omega t)] \tag{E.1}$$

where

$$B_3 = 1/[1 + 2r_2\cos(2\lambda\ell - \theta) + r_2^2] \tag{E.2}$$

$$\eta = 1 + r_2^2 + 2r_2\cos(\theta) \tag{E.3}$$

$$\xi = 2r_2\sin(\theta) \tag{E.4}$$

$$\phi_o = \tan^{-1}[\eta/\xi] \tag{E.5}$$

Let

$$B = \sqrt{\eta^2 + \xi^2} \tag{E.6}$$

and

$$m = B \cdot \sin(\lambda\ell + \phi_o) \tag{E.7}$$

$$n = (r_2^2 - 1)\sin(\lambda\ell) \tag{E.8}$$

Then Equation (E.1) reduces to

$$q^{(o)}(\ell, t) = A \cdot B_3\sqrt{m^2 + n^2}\ [\sin(\omega t + \phi_1)] \tag{E.9}$$

where

$$\phi_1 = \tan^{-1} [n/m] \tag{E.10}$$

Let

$$B_1 = B_3 \sqrt{m^2 + n^2} \tag{E.11}$$

and

$$A_1 = A(B_1) \tag{E.12}$$

Then, Equation (E.7) reduces to

$$q^{(o)}(\ell, t) = A_1 \cdot \sin(\omega t + \phi_1). \tag{E.13}$$

APPENDIX F

SOLUTION FOR $q^{(1)}(x, t)$

From Equation (4.23) we notice that the forcing function has a frequency 2ω; hence, for the response $q^{(1)}(x, t)$ we assume a solution of the form

$$q^{(1)}(x, t) = Je^{i(2\omega t+2\lambda x)} + Ke^{i(2\omega t-2\lambda x)} \tag{F.1}$$

Since the imaginary part of Equation (4.23) is the true forcing function, the imaginary part of $q^{(1)}(x, t)$ will be the actual solution to the set given by Equation (4.5).

From the consideration of the boundary condition at $x = 0$, one obtains

$$J + K = 0 \tag{F.2}$$

Hence, Equation (F.1) reduces to

$$q^{(1)}(x, t) = Je^{i(2\omega t)} \left[(2i)\cdot\sin(2\lambda x)\right] \tag{F.3}$$

Substituting Equation (F.3) in the boundary condition at $x = \ell$ for the set given by Equation (4.5), incorporating Equation (4.23) into this boundary condition, and then solving for the complex constant J, one obtains

$$J = \frac{i\left[\frac{1}{8} c(A_1)^2 \cdot e^{i(2\phi_1)}\right]}{\left[\cos(2\lambda\ell) - 2(\beta c\omega)\sin(2\lambda\ell) + i\{(\alpha c)\sin(2\lambda\ell)\}\right]} \tag{F.4}$$

Substituting for J in Equation (F.3) and considering the imaginary part of $q^{(1)}(x, t)$ to be the true solution, one obtains

$$q^{(1)}(x, t) = -\frac{1}{4} \cdot c \cdot A_1^2 \, (B_2) \cdot \sin(2\lambda x) \cdot \sin(2\omega t + 2\phi_1 + \phi_2) \tag{F.5}$$

where

$$B_2 = [\{\cos(2\lambda\ell) - 2(\beta c\omega) \cdot \sin(2\lambda\ell)\}^2 + \{(\alpha c) \cdot \sin(2\lambda\ell)\}^2]^{-1/2} \tag{F.6}$$

$$\phi_2 = \tan^{-1} \left[\frac{-\alpha c}{\cot(2\lambda\ell) - 2(\beta c\omega)}\right] \tag{F.7}$$

APPENDIX G

EXPRESSIONS FOR THE LINEARIZED LOAD IMPEDANCE OF ORIFICE AND THE DIMENSIONLESS RATIOS ZR1 and ZR2

From Equation (3.20) we have

$$p = L'\dot{q} + K'q^2 + 2K'qq_s. \tag{G.1}$$

Hence, the linearized load impedance of the orifice is

$$Z_\ell = \frac{p}{q} = \frac{1}{q}\left[L'\dot{q} + 2K'qq_s\right]$$

Let

$$q = \mathrm{Im}\left[A\, e^{i\omega t}\right]$$

where Im refers to the Imaginary part of. Then,

$$Z_\ell = 2K'q_s + i(\omega L') \tag{G.2}$$

And for $L' = 0$,

$$Z_\ell = 2K'q_s \tag{G.3}$$

Next, the characteristic impedance of a nonviscous line is given by

$$Z_c = \rho c/(\pi a^2)$$

Now consider the ratio

$$ZR1 = \frac{Z_\ell}{Z_c} = \frac{(2K'q_s)\cdot\pi a^2}{\rho c}$$

$$= \left[\left(\frac{2K'(\pi a^2)}{K_f}\right)\right]\cdot K_f \cdot \frac{q_s}{c} \tag{G.4}$$

Substituting for ε from Equation (3.23), we have

$$ZR = [\varepsilon \cdot \frac{K_f}{\rho} \cdot \frac{q_s}{c}]$$

$$= \varepsilon \, q_s \cdot c$$

Substituting for α from Equation (3.24)

$$ZR = \alpha c \tag{G.5}$$

For a sharp-edge orifice $\alpha = (\alpha 1)$

$$ZR1 = (\alpha 1) \cdot c \tag{G.6}$$

For a short-tube orifice $\alpha = (\alpha 2)$

$$ZR2 = (\alpha 2) \cdot c \tag{G.7}$$

Next, from Equation (G.4),

$$ZR = \frac{2K'(\pi a^2)}{K_f} \frac{K_f}{\rho} \frac{q_s}{c}$$

$$= \frac{2K'(\pi a^2)}{K_f} \cdot c^2 \cdot A_o \cdot M_s \tag{G.8}$$

For a sharp-edge orifice from Equation (3.13),

$$2K' = \frac{\rho}{(C_d \, A_o)^2}$$

$$ZR1 = (\frac{\rho \cdot \pi a^2}{K_f (C_d \, A_o)^2}) \cdot c^2 \cdot A_o \cdot M_s$$

$$= \frac{1}{C_d^2} \cdot (BCP1) \tag{G.9}$$

Next, for a short-tube orifice, from Equation (3.14),

$$2K' = \frac{\rho}{(C_d \, A_o)^2} + \frac{\rho f L}{D_o \, A_o^2}$$

Substituting for 2K' in Equation (G.8),

$$ZR2 = \left(\frac{\pi a^2}{K_f}\right)\cdot\left[\frac{\rho}{(C_d A_o)^2} + \frac{\rho f L}{D_o A_o^2}\right] c^2 \cdot A_o \cdot M_s$$

$$= \left[\frac{1}{C_d^2} + f\left(\frac{L}{D_o}\right)\right]\cdot\left(\frac{\pi a^2}{A_o}\right)\cdot M_s$$

$$= \left[\frac{1}{C_d^2} + f\left(\frac{L}{D_o}\right)\right]\cdot BCP1. \qquad (G.10)$$

APPENDIX H

LISTINGS OF COMPUTER PROGRAMS

```
      C
      C  PROGRAM TO COMPUTE THE AMPLITUDE RATIO FUNDAMENTAL (ARFUND) THE PERCENTAGE
      C  SECOND HARMONIC DISTORTION (PSHDIS), THE PHASE ANGLE OF THE FUNDAMENTAL
      C  (PHI1) AND THE PHASE ANGLE OF THE SECOND HARMONIC (PHI3) AS FUNCTIONS OF THE
      C  FREQUENCY NUMBER 'FN' (FOR GIVEN VALUES OF THE BOUNDARY CONDITION PARAMETERS
      C  BCP1 AND BCP21 ). THIS PROGRAM WORKS FOR NONZERO VALUES OF BCP21 AND FN.
      C  ASSIGNMENT OF A ZERO VALUE TO EITHER BCP21 OR FN WILL LEAD TO A 'DIVIDE CHECK
      C  ERROR' IN THE INTERNAL STATEMENT NUMBERS 28 AND 46 RESPECTIVELY. THE RESULTS
      C  OF STRUNK ARE READILY OBTAINED BY CONSIDERING SMALL NONZERO VALUES FOR THE
      C  PARAMETER BCP21.
      C
      C
 1          DATA ICNT,JCNT,CD,XL,BCP21,AQ/0,0,0.6,1.0,0.001,0.5/
 2          PI=3.14159
 3        5 BCP1=0.1
 4       10 ZR1=(BCP1)/((CD)**2)
 5       15 WRITE(6,20)BCP1,BCP21
 6       20 FORMAT(1HO,'BCP1 =',1X,F4.2,5X,'BCP21 =',1X,F10.8)
 7          WRITE(6,25)
 8       25 FORMAT(1HO,5X,'FN',13X,'ARFUND',11X,'PSHDIS',12X,'PHI1',13X,'PHI3'
           $)
 9          DO 45 L=1,7
10          IF(L-1)26,26,27
11       26 FN=0.025
12          GO TO 30
13       27 FN=FLOAT(L-1)
14       30 RO=(1.0-((ZR1)**2)-((BCP21)**2))
15          R1=SQRT(((RO)**2)+4.0*((BCP21)**2))
16          DNR1=((1.0+(ZR1))**2)+((BCP21)**2)
17          R2=R1/DNR1
18          IF(ZR1-1.0)32,32,31
      C
      C  THIS CHECK COMES INTO EFFECT WHEN BCP1 CROSSES THE TRANSITION VALUE OF 0.36.
      C  IT IS ASSUMED THAT THE PARAMETER BCP21 REMAINS (NUMERICALLY) LESS THAN UNITY.
      C  FOR VALUES OF 'BCP1' GREATER THAN 0.36, 'ZR1' IS GREATER THAN UNITY,AND FOR
      C  'BCP21' REMAINING LESS THAN UNITY, THE SIGN OF 'RO' IS GOVERNED BY THE VALUE
      C  OF 'ZR1'.
      C       NOTICE FOR BCP21=0.0 AND 'ZR1' GREATER THAN UNITY, THE ARGUMENT OF THE
      C  'SQRT' DEFINING 'R1' IS A PERFECT SQUARE OF A NEGATIVE NUMBER. THEREFORE 'R1'
      C  IS A NEGATIVE NUMBER AND SO IS 'R2'.
      C         FOR LESS THAN UNITY, POSITIVE NONZERO VALUES OF 'BCP21' THE ARGUMENT OF
      C  'SQRT' DEFINING 'R1' IS NOT A PERFECT SQUARE. HOWEVER, IF THE TERM (4.0*(
      C  BCP21)**2) IS SMALL COMPARED TO THE SQUARE OF 'RO', THEN IT MAY BE NEGLECTED
      C  AND ONLY FOR SUCH CASES THE SIGN OF 'R1' (AND 'R2') CONTINUES TO BE GOVERNED
      C  BY THE VALUE OF 'ZR1'.
      C
19       31 R2=-R2
20       32 THETA=ATAN((-2.0*(BCP21))/(1.0-((ZR1)**2)-((BCP21)**2)))
21          DNR2=1.0+(2.0*R2*COS((2.0*FN)-THETA))+((R2)**2)
22          B3=1.0/DNR2
23          AX=(((R2)**2)-1.0)*(SIN(FN*XL))
24          BX=DNR2*(COS(FN*XL))+(2.0*R2*(SIN((2.0*FN)-THETA))*(SIN(FN*XL)))
25          CX=SQRT(((AX)**2)+((BX)**2))
26          ETA=1.0+((R2)**2)+2.0*R2*COS(THETA)
27          ZETA=2.0*R2*SIN(THETA)
28          PHIO=ATAN(ETA/ZETA)
29          ETASQ=(ETA)**2
30          ZETASQ=(ZETA)**2
```

```
      B=SQRT(ETASQ+ZETASQ)
      IF(ZETA)33,34,34
   33 SAI=FN-PHIO
      GO TO 35
   34 SAI=FN+PHIO
   35 XM=B*SIN(SAI)
      XN=(((R2)**2)-1.0)*SIN(FN)
      SQM=((XM)**2)
      SQN=((XN)**2)
      B4=((ZR1)*SIN(2.0*FN))**2
      B2=1.0/(SQRT(((COS(2.0*FN)-2.0*(BCP21)*SIN(2.0*FN))**2+B4))
      B1SQ=(SQM+SQN)*((B3)**2)
      ARFUND=(B3)*(CX)
      PSHDIS=ABS(((25.0)*AQ*ZR1*B1SQ*B2*SIN(2.0*FN*XL))/(B3*CX))
      PHI1=ATAN(XN/XM)
      PHI2=ATAN((-ZR1)/((1.0/(TAN(2.0*FN)))-2.0*(BCP21)))
      PHI3=(2.0*PHI1)+PHI2
      PHI1D=(PHI1*180.0)/(PI)
      PHI2D=((PHI2)*180.0)/(PI)
      PHI3D=(PHI3*180.0)/(PI)
      IF(PHI1D)36,37,37
   36 PHI1D=PHI1D+360.0
   37 IF(PHI3D)38,39,39
   38 PHI3D=PHI3D+360.0
   39 WRITE(6,40)FN,ARFUND,PSHDIS,PHI1D,PHI3D
   40 FORMAT(1H0,F10.5,10X,F5.2,10X,F7.2,10X,F7.2,10X,F7.2)
      IF(FN-6.0)41,46,46
   41 FN=FN+0.025
      JCNT=JCNT+1
      IF(JCNT-39)30,30,42
   42 JCNT=0
   45 CONTINUE
   46 BCP21=BCP21*1.5
      IF(BCP21-0.5)15,15,50
   50 BCP21=0.001
      ICNT=ICNT+1
      BCP1=(BCP1)*10.0
      IF(ICNT-1)10,10,55
   55 STOP
      END
```

```
      C
      C  PROGRAM TO EVALUATE THE AMPLITUDE RATIO FUNDAMENTAL (ARFUND) AND THE PERCEN-
      C  TAGE SECOND HARMONIC DISTORTION (PSHDIS) AS FUNCTIONS OF THE AXIAL POSITION
      C  NUMBER 'XL', FOR GIVEN NONZERO VALUES OF THE FREQUENCY NUMBER 'FN' AND THE
      C  BOUNDARY CONDITION PARAMETER 'BCP21'.
      C
      C
 1        DATA ICNT,JCNT,CD,BCP1,BCP21,AQ/0,0,0.6,1.0,0.25,0.5/
 2     5  FN=1.6
 3     10 ZR1=(BCP1)/((CD)**2)
 4     15 WRITE(6,20)FN,BCP1,BCP21
 5     20 FORMAT(1HO,'FN =',1X,F4.2,5X,'BCP1 =',1X,F5.2,5X,'BCP21 =',1X,
         $F10.8)
 6        WRITE(6,25)
 7     25 FORMAT(1HO,'XL',10X,'ARFUND',10X,'PSHDIS')
 8        XL=0.0
 9     30 RO=(1.0-((ZR1)**2)-((BCP21)**2))
10        R1=SQRT(((RO)**2)+4.0*((BCP21)**2))
11        DNR1=((1.0+(ZR1))**2)+((BCP21)**2)
12        R2=R1/DNR1
13        IF(ZR1-1.0)32,32,31
      C
      C  THIS CHECK COMES INTO EFFECT WHEN BCP1 CROSSES THE TRANSITION VALUE OF 0.36.
      C  IT IS ASSUMED THAT THE PARAMETER BCP21 REMAINS NUMERICALLY LESS THAN UNITY.
      C  FOR VALUES OF 'BCP1' GREATER THAN 0.36, 'ZR1' IS GREATER THAN UNITY,AND FOR
      C  'BCP21' REMAINING LESS THAN UNITY, THE SIGN OF 'RO' IS GOVERNED BY THE VALUE
      C  OF 'ZR1'.
      C        NOTICE FOR BCP21=0.0 AND 'ZR1' GREATER THAN UNITY, THE ARGUMENT OF THE
      C  'SQRT' DEFINING 'R1' IS A PERFECT SQUARE OF A NEGATIVE NUMBER. THEREFORE 'R1'
      C  IS A NEGATIVE NUMBER AND SO IS 'R2'.
      C        FOR LESS THAN UNITY, POSITIVE NONZERO VALUES OF 'BCP21' THE ARGUMENT OF
      C  'SQRT' DEFINING 'R1' IS NOT A PERFECT SQUARE. HOWEVER, IF THE TERM (4.0*(
      C  BCP21)**2) IS SMALL COMPARED TO THE SQUARE OF 'RO', THEN IT MAY BE NEGLECTED
      C  AND ONLY FOR SUCH CASES THE SIGN OF 'R1' (AND 'R2') CONTINUES TO BE GOVERNED
      C  BY THE VALUE OF 'ZR1'.
      C
14     31 R2=-R2
15     32 THETA=ATAN((-2.0*(BCP21))/(1.0-((ZR1)**2)-((BCP21)**2)))
16        DNR2=1.0+(2.0*R2*COS((2.0*FN)-THETA))+((R2)**2)
17        B3=1.0/DNR2
18        AX=(((R2)**2)-1.0)*(SIN(FN*XL))
19        BX=DNR2*(COS(FN*XL))+(2.0*R2*(SIN((2.0*FN)-THETA))*(SIN(FN*XL)))
20        CX=SQRT(((AX)**2)+((BX)**2))
21        ETA=1.0+((R2)**2)+2.0*R2*COS(THETA)
22        ZETA=2.0*R2*SIN(THETA)
23        PHI0=ATAN(ETA/ZETA)
24        ETASQ=(ETA)**2
25        ZETASQ=(ZETA)**2
26        B=SQRT(ETASQ+ZETASQ)
27        IF(ZETA)33,34,34
28     33 SAI=FN-PHI0
29        GO TO 35
30     34 SAI=FN+PHI0
31     35 XM=B*SIN(SAI)
32        XN=(((R2)**2)-1.0)*SIN(FN)
33        SQM=((XM)**2)
34        SQN=((XN)**2)
35        B4=((ZR1)*SIN(2.0*FN))**2
36        B2=1.0/(SQRT((COS(2.0*FN)-2.0*(BCP21)*SIN(2.0*FN))**2+B4))
37        B1SQ=(SQM+SQN)*((B3)**2)
38        ARFUND=(B3)*(CX)
39        PSHDIS=ABS(((25.0)*AQ*ZR1*B1SQ*B2*SIN(2.0*FN*XL))/(B3*CX))
40        WRITE(6,36)XL,ARFUND,PSHDIS
41     36 FORMAT(1HO,F5.2,10X,F5.2,10X,F7.2)
42        XL=XL+0.1
43        JCNT=JCNT+1
44        IF(JCNT-10)30,30,40
45     40 JCNT=0
46        BCP21=BCP21*1.5
47        IF(BCP21-0.5)15,15,50
48     50 BCP21=0.001
49        ICNT=ICNT+1
50        BCP1=(BCP1)*10.0
51        IF(ICNT-1)10,10,55
52     55 STOP
53        END
```

VITA

K. Vijay Kumar Pillai

Candidate for the Degree of

Master of Science

Thesis: FREQUENCY RESPONSE OF FLUID TRANSMISSION LINES WITH A NONLINEAR BOUNDARY CONDITION

Major Field: Mechanical Engineering

Biographical:

Personal Data: Born in Nagpur, Maharashtra, India, August 26, 1947, the son of Mr. and Mrs. R. Krishnaswamy Pillai.

Education: Graduated from St. Gabriel's High School, Warangal, A.P. India, in March, 1965; attended the Regional Engineering College, Warangal; received the Bachelor of Engineering degree in Mechanical Engineering from Osmania University in 1971, attended subsequently the Indian Institute of Science and completed the requirements for the degree of Master of Engineering (Machine Design) in August, 1973.

Professional Experience: Graduate research assistant, School of Mechanical Engineering (Fluid Power Research Center), Oklahoma State University, 1973-75, studying the flow-induced transverse vibration of a hydraulic transmission line under steady flow conditions, the bending vibrations of hydraulic transmission line with time-dependent boundary conditions, hydraulic conduit noise reduction through vibration absorption and the fatigue failure of hydraulic system components; Project Engineer for the research sponsored by the Caterpillar Tractor Co., Peoria, Illinois, to analyze the transmission of liquid-borne noise in hydraulic transmission lines under steady oscillatory flow conditions.

Professional Affiliation: Student Member, The American Society of Mechanical Engineers until December, 1975, thenceforth an Associate Member.